

https://dspace.org/

Theoretical study of flux compression for the conceptual design of a non-explosive FCG

Dickson, Andrew Stuart

2006-10-31T09:59:45Z
http://hdl.handle.net/10539/1521

Downloaded from a DSpace repository. https://dspace.org/

Theoretical study of flux compression for the conceptual design of a non-explosive FCG

Andrew Stuart Dickson

A dissertation submitted to the Faculty of Engineering and the Built Environment, University of the Witwatersrand, Johannesburg, in fulfilment of the requirements for the degree of Master of Science in Engineering.

Johannesburg, August 2005

Declaration

I declare that this dissertation is my own, unaided work, except where otherwise acknowledged. It is being submitted for the degree of Master of Science in Engineering in the University of the Witwatersrand, Johannesburg. It has not been submitted before for any degree or examination in any other university.

Signed this __ day of _____ 20__

_____

Andrew Stuart Dickson.

Abstract

The history of flux compression is relatively short. One of the founders, a Russian physicist, Sakharov developed the idea of compressing a magnetic field to generate high magnetic fields and from this he also developed a generator to produce current impulses. Most of this initial work was performed in military research laboratories. The first open source literature became available in the 1960s and from there it has become an international research arena. There are two types of flux compression generators, field generators and current generators. These are discussed along with the basic theory of flux compression generators and related physics. The efficiency of generators is often quite low. However in many generators high explosives are used and because of their high energy density, the current or field strength produced is substantially greater then the initial source. This of course limits the locations possible for experimental work and subsequently limits the industrial applications of flux compression generators .

This research presents a theoretical design for a non-explosive flux compression generator. The generator is designed to produce a current impulse for tests in laboratory and remote locations. The generator has the advantage of being non-destructive, therefore reducing costs, and allowing for repeatable experiments. The design also reduces the possibilities or many of the loss mechanisms.

Dad, Mom and the family, thank you for love and support.

To Lara my one and only.

Acknowledgements

Thanks to Profesor Ian Jandrell, for introducing me to this strange and interesting subject and for the guidance shown during this research and to Jeoffrey Turner at NECSA for some sound advice.
The author would like to acknowledge Eskom for their support through TESP as well as DTI funding received through THRIP and NRF.

Contents

Declaration **i**

Abstract **ii**

Acknowledgements **iv**

Contents **v**

List of Figures **xi**

List of Tables **xiv**

Preface **xiv**

MSc paper **1**

Introduction **9**

Appendix A **11**

A.1 A history of flux compression 11

A.1.1 Typical areas of use 13

A.2 Modern pulsed power 16

A.2.1 Flux compression with high temperature superconductors 16

A.3 Summary 17

Appendix B **18**

B.1 Physical processes and definitions 18

B.1.1 Magnetic flux 18

B.1.2 Energy stored in a magnetic field 21

B.1.3 LR Circuit 22

B.2 Inductance 22

B.3 Self – Inductance 23

B.3.1 Finite-length solenoid 24

B.4 Mutual – Inductance 24

B.5 Mechanical characteristics 26

B.5.1 Characteristic gas equations 26

B.5.2 Projectile energy 27

B.5.3 Projectile velocity 27

B.6 Summary 29

Appendix C **30**

C.1 Flux 30

C.1.1 What is Flux? 30

C.1.2 Energy available in flux compression – energy in a magnetic field 31

C.2 The Ideal Flux compressor – some basic theory 31

C.3 Equivalent circuit for current generators 33

C.3.1 Flux compression by incompressible plane conductors . . 35

C.4 Magnetic flux compression by a rod and rail system 36

C.4.1 Rod and rail design analysis 41

C.5 Implosion of a cylindrical ideal flux compressing shell 44

C.6 Types of flux compressors 45

C.6.1 Sakharov's MK-1 generator 46

C.6.2 Sakharov's MK-2 generator 47

C.6.3 Explosive flux compression 48

C.6.4 Electromagnetic implosive devices 48

C.7 Flux compression - according to Levi 51

C.7.1 Initial field generation 51

C.7.2 Flux compression 52

C.8 High-Voltage MCG systems 53

C.8.1 Magnetic flux trapping 53

C.9 The use of transformers on electrical loads 54

C.9.1 Direct connection to a load 54

C.9.2 Connection through pulsed transformers 55

C.10 Summary 57

Appendix D **58**

D.1 FLEXY I Design, construction and testing 58

D.2 FLEXY I Computer models 59

D.2.1 A simple general model for a helical MCG 60

D.2.2 Simple 2D model for a Helical MCG 69

D.3 Helical generator design 74

D.3.1 HFCG Parameters 74

D.3.2 Design rules 75

D.4 Network mesh model for a FCG 75

D.5 Summary 76

Appendix E **78**

E.1 Measurement devices 78

E.1.1 Magnetic measurement devices 78

E.1.2 Current measurement devices 79

E.1.3 Mechanical measurement devices 80

E.1.4 Measuring limitations 81

E.2 Summary 81

Appendix F **82**

F.1 Losses 82

F.2 Magnetic losses 83
F.2.1 Flux diffusion 83
F.2.2 Magnetic forces 84
F.2.3 Flux pockets 84
F.3 Thermal losses 84
F.3.1 Eddy current losses - temperature rise 84
F.4 Electrical losses 85
F.4.1 High electric fields - electrical breakdown/arcing 85
F.5 Mechnical losses 85
F.5.1 Mechanical defects 85
F.5.2 Turn skipping or π-clocking 86
F.5.3 Liner destruction 86
F.6 Dealing with these problems 86
F.6.1 Gas in generator volumes 87
F.7 Summary 87

Appendix G **88**

G.1 Non-explosive magnetic compression generator 88
G.2 The design 90
G.2.1 Two stage light gas gun 91
G.2.2 Flux compression generator design 91

G.3 Design advantages 92

G.4 Summary 93

References **94**

List of Figures

A.1 Operation of the AKEM magnetic flux compression projectile [6]. 15

B.1 A conducting rod moving on a U-shaped conductor in a uniform magnetic field [14]. 20

B.2 The current rise within a conductor. 22

B.3 The flux linkage of a single turn current carrying coil. 23

B.4 The mutual inductance between two loops. 25

C.1 Field conservation by varying a conductors area [5]. 31

C.2 Graph showing the relationship of β to the current gain (G_I) of a flux compression generator. 32

C.3 Equivalent circuit diagram of a flux compression generator [4]. . 33

C.4 Parallel plane compression system [4]. 35

C.5 Rod and rails system used in Namias's work [24]. 37

C.6 A graph showing the relationship of the initial velocity of the rod to the maximum field obtainable and the turn around position of the rod. 42

C.7 Graph showing the velocity of the rod as it approaches the turn around point. 43

C.8 Graph of the maximum field and the turn around point in relation to the initial field strength. 43

C.9 Graph showing curves relating to different initial rod velocities for a varying initial magnetic field. 44

C.10 An ideal shell (a) before and (b) during implosion [4]. 45

C.11 Diagram of the MK-1 generator. 47

C.12 Diagram of the MK-2 generator [1]. 47

C.13 θ – implosion generator set-up [4]. 49

C.14 z – implosion generator set-up [4]. 50

C.15 Seed field circuit. 52

C.16 Circuit including a crowbar switch and a graph showing the time varying inductance over time. 52

C.17 Equivalent circuit diagram for an MCG [23]. 55

C.18 Equivalent circuit diagram for MCG connected through a pulsed transformer to a complex load [23]. 56

D.1 FLEXY I schematic (a) before detonation and (b) during detonation [23]. 59

D.2 A four-section generator [23]. 61

D.3 The effects of geometric defects and the occurrence of voltage breakdown [23]. 68

D.4 Decomposition of a helical generator into z and θ circuits [23]. . 70

D.5 Equivalent circuit diagram with the armature separated into θ rings. 71

D.6 Generator schematic for a network mesh model [29]. 76

E.1 Rogowski coil and integrating circuitry [31]. 80

G.1 Graph showing the field strength during flux compression. . . . 89

G.2 Schematic of non-explosive flux compression generator design. . 90

G.3 Diagram of the liner to be used in the generator. 91

List of Tables

B.1 Coefficients of kinetic friction for metals. 27

C.1 Results from electromagnetic implosion generators. 51

Preface

The format of this Masters dissertation differs from the conventional format in that it comprises a short body (in the form of a paper) followed by a number of appendices. The substance of the project is in the appendices. It is recommended that the paper entitled "The fundamentals of flux compression - theoretical discussion of a non-explosive current generator " is reviewed first to gain an understanding of the work performed.

The appendices provide information about the history of flux compression, development of fundamental theory and model design. This is finally compiled in a theoretical design of a flux compression generator designed for impulse generation. The following is a brief summary of the contents of each of the appendices.

Appendix A - Looks into the history of flux compression including the past and present researchers. Some modern day application of flux compression generators are also reviewed.

Appendix B - Introduces the fundamental physics and electrical theory required for the understanding of flux compression. Particular areas of importance include the magnetic theory and processes used in determining self and mutual inductances.

Appendix C - Reveals the fundamental theory of flux compression generators. Theory based on ideal and non-ideal generators is presented. Different flux compression techniques are reviewed and the equivalent circuits are discussed.

Appendix D - Introduces two generator models created at Loughborough University, UK, by Novac and Smith are presented. A simple model is initially presented and then a complex 2D model for a helical flux compression generator

is discussed.

Appendix E - Discusses the measurement systems required in many experiments performed on flux compression generators. These tools are used to verify the models developed to help make the models more accurate.

Appendix F - Highlights the four main loss areas that a flux compression generator can experience. Some methods to reduce the losses are also explained in this appendix.

Appendix G - Discusses the theoretical design of a non-explosive flux compression generator. The advantages this system has over conventional explosive flux compression generators is also discussed.

THE FUNDAMENTALS OF FLUX COMPRESSION - THEORETICAL DISCUSSION OF A NON-EXPLOSIVE CURRENT GENERATOR

A. S. Dickson*

**University of the Witwatersrand, Department of Electrical and Information Engineering, RSA*

Abstract. A result of military research flux compression generators have been investigated since the 1950s, the USSR and America both working on generator designs in military research laboratories. Sakharov of the USSR was the father of two designs which are both still in use today, the MK-1 and MK-2 flux compression generators. Generators are designed for the generation of either high magnetic fields or high current impulses. The fundamental theories of flux compression generators are reviewed as well as a description of electromagnetic and explosive generator designs. In most generator designs very large capacitor banks are needed and in most designs of current impulse generators high explosives are also required. This limits the facilities and location for the use of flux compression generators. With the understanding of the losses experienced in a generator volume the design of a non-explosive generator is discussed. This highlights methods to reduce losses in a generator design as well as making the generator portable.

Key Words. Flux compression, High explosives, Electromagnetic compression, Current generator

1 INTRODUCTION

For the last 50 years flux compression has been developed and studied. Initial work was performed in classified laboratories because of its military nature. The late 1960s saw some of the first open literature on the subject of flux compression. Two of the most recognised works on the subject were published in 1970, a paper written by Erber and Latal [1] discussing the theories of flux compression and a book written by Heinz Knoepfel [2] about magnetic theory including a section on flux compression generators. Development of the subject has grown extensively since then with international conferences and inter-lab experiments being performed.

Generators are designed with one of two purposes, either for the generation of high magnetic fields or the production of large current impulses. The generators rely on two processes for effective operation, a high change of inductance (dL/dt) and a large energy density source. The energy source is usually in the form of high explosives (HE) or a large capacitor bank. The field in a generator is usually compressed by either a collapsing liner or armature or by the expansion thereof. In most cases the liner should have a velocity of at least a 1000 ms^{-1} or faster; this is to prevent unnecessary flux leakage out of the generator.

This paper will look at the history of flux compression and initial design concepts. The fundamental components will be addressed and the corresponding system losses will be presented. Finally a design for a non-explosive flux compression generator for the production of a current impulse will be presented and discussed.

2 HISTORY

There is some debate as to the origin of flux compression. During the second world war research was being performed in the United States as well as USSR. Joseph Fowler performed the initial work on flux compression at the *Los Alamos Laboratory* in the USA in 1944 [2]. A. Sakharov performed work at the *Kurchatov Institute* proposing the concept of imploding liners to compress magnetic flux. A collection of his scientific works were finally published in

1982 [3]. Details of his initial design of the MK-1 and MK-2 devices will be discussed in this paper. Most designs that are produced these days are related to one of these designs of Sakharov.

In 1961 the first conference on the generation of high magnetic fields was held in Boston [2]. This conference looked at the development of high magnetic fields by any means. New developments were being made by 1966 in the generation of high magnetic fields using capacitor banks and imploding liners (foils) by Cnare in the USA.

This eventually led to the publishing of two comprehensive works on magnetic flux compression. The first was a paper written by T. Erber and H. G. Latel, titled "Flux compression theories" [1]. This work is the starting point for most work performed in flux compression these days. It covers aspects of both explosive and electromagnetic flux compression. It also introduces some theory about ideal flux compression. The second is a book written by Heinz Knoepfel called "Pulsed magnetic fields" [2], providing an in-depth look at magnetic fields and the theories surrounding magnetic fields and their interaction with conductors. A second book published in 2000 written by Knoepfel called "Magnetic fields" [4] is very similar to his initial book, but it is a far more comprehensive, with many more years of research included.

In the early 1990s the governments of the USA and Russia promoted lab-to-lab interactions. This interaction was performed between the *All-Russian scientific Research Institute of Experimental Physics (VNIIEF)* and the *Los Alamos National Laboratory (LANL)*. Initial work was performed on the Russian DEMG (Disk explosive magnetic generator) which has unmatched performance in terms of output current and energy [5]. The interaction between these labs has produced over 15 experiments performed between the two institutions and has allowed for great advancements in the understanding of flux compression.

Many research facilities around the world are performing work in flux compression; these include Japan, China, Poland, France, UK and South Africa. A lot of the most prominent current work is coming from Loughborough University in the UK, by I.R. Smith and B.M. Novac. Together they have developed 2-D and 3-D models for helical flux-compression generators [6–8]. Many of the papers produced by Novac, Smith, Altgilbers and Tkach are published in a book called "Magnetocumulative generators" [8]. The book deals with many aspects of magnetocumulative generators from the the different types, designs, loads and measuring equipment used.

Flux compression generators (FCGs) are being used in a greater number of fields of research with some industrial applications. Historically FCGs were used mainly in physics experiments dealing with charged particle diodes and imploding plasma. The main area of use was in military applications which to a large extent are still restricted. Modern day uses include biological, biomedical and environmental applications with two industrial applications in the form of oil and mineral exploration as well as land mine detection. The work on land mine detection is being performed in Missouri, USA. The flux compression generator is housed in a projectile which on impact, an anvil mass compresses the volume. This propagates an electromagnetic wave through the soil which exposes landmines which can be seen on a radar screen [9].

3 THE FUNDAMENTAL CONCEPTS

Flux compression in the ideal case relies on Faraday's law of flux conservation. This is best demonstrated by the diagram shown in *figure 1*: if the area changes the flux density B_F must increase [5].

$$\mathbf{B}_i A_i = \mathbf{B}_f A_f \tag{1}$$

$$\phi_i = \phi_f \tag{2}$$

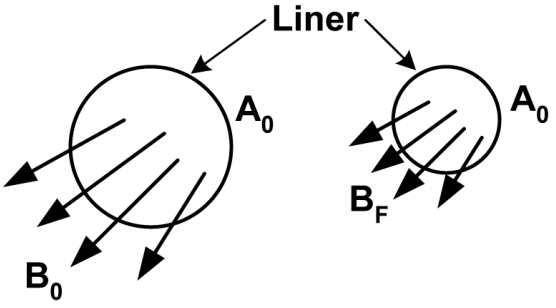


Figure 1. Conservation of flux by Faraday's law

This can be rewritten in terms of the current and inductance of the generator.

$$L_i i_i = L_f i_f \tag{3}$$

From these two equations two things can be noted. In order to obtain a high magnetic field

the moving liner should have as high a velocity as possible to prevent the dissipation of the flux through the liner therefore causing losses in the system. For a high current output there should be a large initial inductance of the system and the final inductance should be as low as possible. The final inductance includes the load which in some cases requires the generator to be coupled to the load via a transformer. A lot of work performed with FCGs requires the calculation of the mutual inductances of the generator. The most common method used for these calculations is by using standard elliptic integrals $K(k)$ and $E(k)$ [10, 11].

The energy component of the system comes from two main sources, these are defined in *equation 4 & 5*. The energy equations are written for a cylindrical system. The first is the initial energy in the magnetic field produced either by permanent magnets or by a capacitor bank and coil.

$$U = \frac{1}{2}LI^2 \quad or \quad U = \frac{1}{2}\mu_0 H^2 \pi R^2 \tag{4}$$

In this equation R is the internal radius of the cylinder. The second source is from the mechanical movement of the liner whether it be from a HE detonation or from an electromagnetic source. The energy of the liner is defined by:

$$KE = \frac{1}{2}mv^2 \quad or \quad KE = \pi\rho^2 v_0^2 R_1^2 ln\left(\frac{R_2}{R_1}\right) \tag{5}$$

R_1 and R_2 in *equation 5* are for the internal and outer radii respectively. In the ideal case all of the kinetic energy will be converted into magnetic energy in the field which is then used either as a high magnetic field source or converted into electrical energy.

4 FLUX COMPRESSION GENERATORS

There are two classes of flux compression generators [8]:

- High-energy density or field generators, generating high magnetic fields
- Current or energy generators, current generation for separate inductive loads

The generation of high magnetic fields is produced in two ways, the use of HE to compress a cylinder generating the high fields or by electromagnetic compression. The generation of current is in most cases produced by HE.

4.1 Field generators

As mentioned earlier there are two types of generator designs for the production of high magnetic fields. The first design was produced by Sakharov and called the MK-1. Designed with HE wrapped around a liner which when detonated compressed the liner and therefore compressed the field. The initial experiments performed in 1952, yielded fields of 100 Tesla from an initial field of 3 Tesla [3]. As can be seen in *figure 2* there is a

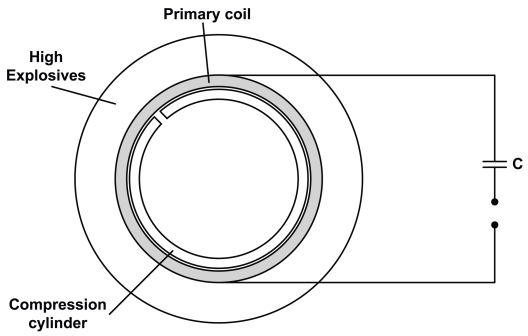


Figure 2. Diagram of Sakharov's MK-1 generator

slit in the compression cylinder. This allows for a faster penetration of the initial field into the middle of the compression cylinder. On detonation of the liner this gap is closed and the flux is trapped and compressed.

The second method for the production of high magnetic fields is by electromagnetic compression of a liner. This system is usually a single turn coil with a liner placed inside the coil. In some cases the imploding liner is placed in a vacuum to reduce air friction and shock waves. There are two set-ups generally used for electromagnetic flux compression. They are ϕ-implosion and z-implosion, ϕ-implosion is shown in *figure 3*. As can be seen in the figure the currents for the compression of the liner only flow in the stator section. The field produced by this are parallel to the z-axis. The generated field induces a current in the liner and because of this there is repulsion between the stator and the liner and the liner is concentrically compressed [1].

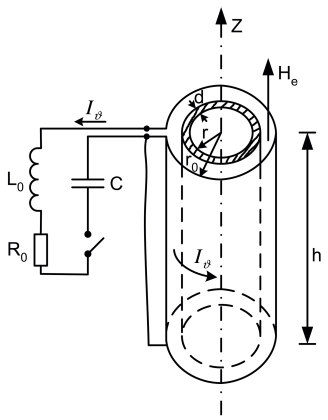


Figure 3. ϕ-implosion generator set-up [4]

In the case of z-implosion systems instead of the current flowing in the outer stator section only, the capacitor bank is connected to the liner and the stator, causing a circular field perpendicular to the z-axis. The same principle applies, because of the currents flowing in opposite directions in the stator and liner. Fields generated by Knoepfel using electromagnetic compression generators are shown in *table 1.*

	ϕ-implosion	z-implosion
Capacitor energy	136 kJ	570 kJ
Initial field	2.5 T	3.5 T
Implosion velocity	0.17 cm/μs	0.13 cm/μs
Maximum field	110 T	280 T

Table 1. Electromagnetic implosion results recorded by Knoepfel [2]

For Electromagnetic compression large capacitor banks are needed to obtain results as shown in *table 1.* In both cases the implosion equation of motion is described by:

$$-m\frac{d^2r}{dt^2} = \frac{1}{2}\mu H^2 2\pi r \tag{6}$$

4.2 Current generators

The MK-2 generator design by Sakharov is still one of the most popular designs for a current or energy generator. *Figure 4* shows the basic components of the generator. HE has a very large specific energy density which in the ideal case would create incredibly high current impulses. However in real world applications the efficiency of these devices is usually not more than 20-30%. Even though this is the case there is still an incredibly large impulse that is created from an initially small current.

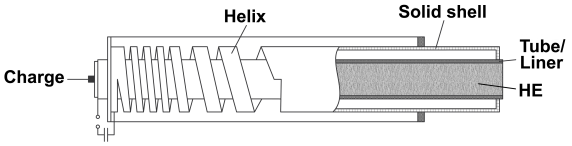


Figure 4. Diagram of Sakharov's MK-2 generator

4.2.1 Equivalent circuit The fundamental circuit is found in quite a few variations, but in all cases operates in a similar manner [1, 4, 8, 12]. Knoepfel's equivalent circuit is shown in *figure 5.* The dotted section defines the seed current branch of the generator. Once the current has been delivered to the generator a crowbar shorts out the seed current circuit. L_c describes the time changing inductance of the generator. The resistance,

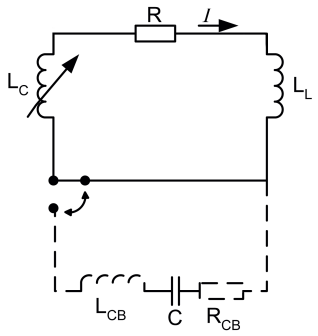


Figure 5. Equivalent circuit diagram for a flux compression generator [4]

R, defines the magnetic flux losses of the generator and the generated impulse is delivered to the load, L_L. The circuit is defined by the differential equation:

$$\frac{d(LI)}{dt} + RI = 0 \tag{7}$$

Solving this equation provides a solution for the system at any instant in time, defined by:

$$LI = L_0 I_0 \exp\left\{ -\int_0^t \frac{R}{L} dt \right\} \tag{8}$$

L_0 is the total initial inductance at time equal to zero. I_0 is the initial seed current delivered to the generator.

5 ASSOCIATED LOSSES

The calculations used in an ideal FCG provides a workable solution. There is however a large discrepancy between the ideal and real cases because of the associated losses of a generator. There are methods to reduce these losses; however in some cases a minor flaw can have a devastating effect on the results from a generator. There are four main types of losses of an FCG, which are:

- Magnetic
- Mechanical
- Thermal
- Electric

The losses overlap each other and reducing one often reduces others. However it is not possible to remove all the losses.

5.1 Flux diffusion

Flux diffusion is probably the most important loss characteristic to have as small as possible. If the conductivity of the conductor is very high its performance is more like a lossless system. Work done using different conductors has shown that the dif-

ference in performance between a copper and aluminium conductor is only a few percent. The diffusion of flux occurs when the conductor is compressing the flux and the flux penetrates through the conductor. The rate at which this penetration occurs is affected by the finite resistivity (ρ) of the conductor and the velocity (v) at which the conductor is moving. Erber and Latal [1] defined a value for the velocity of the liner in order ot be able to compress flux. The equation defining the velocity is:

$$v \simeq \frac{\left|a_i^{1/2} - a_f^{1/2}\right|}{\tau_0} \tag{9}$$

Where τ is defined as:

$$\tau_0 = \frac{\mu_0 \delta r}{2\rho} \tag{10}$$

For thick walled conductors the whole system is non-uniform. The current density is non-uniform, which in turn makes the heating non-uniform and therefore the change of conductivity is non-uniform. The skin layer for a conductor is defined by:

$$\delta = \sqrt{\frac{2}{\omega \mu \sigma}} \tag{11}$$

Associated with this is the skin time, which is the time required for the magnetic field to penetrate the conductor to the depth of the skin layer. This is defined as:

$$\tau_s = \frac{1}{2}\pi \sigma \delta^2 \tag{12}$$

All these values aid in the design of a generator, often setting the minimum values required for flux compression to occur. Of course without sufficient flux being held in the compression volume, the output will be negligible.

5.2 High electric fields - electrical breakdown

A conductor moving through a magnetic field will generate an electric field on its surface defined by:

$$\boldsymbol{E} = -v \times \boldsymbol{B} \tag{13}$$

In many cases the magnetic field and moving liner are not parallel to each other and therefore the electric field generated is defined by:

$$\mathbf{E} = \frac{v\mathbf{B}}{\sin\,\alpha} \tag{14}$$

Electrical breakdown therefore usually occurs just before the liner and stator touch, aided by a small angle and high field. Any flux that has been compressed prior to the electrical breakdown will be lost from the rest of the compression process. SF_6 can be introduced into the compression volume in order to reduce the chances of electrical breakdown [8].

5.3 Turn skipping - π-clocking

This loss is primarily related to the skipping of turns as the liner makes contact with the stator. This is as a result of the misalignment of the liner and stator sections. In most helical generators this often occurs in the earlier sections of the compression as the windings are quite close together. Through their work, Altgilbers et al. [8] consider turn skipping to be the most important loss mechanism that needs to be considered.

Additional loss mechanisms that play some part in the deterioration of a generators performance will be briefly discussed. In most cases because of a minor loss mechanism one of the losses mentioned before will be the final result. Machining defects often lead to uneven surfaces which are amplified under explosive conditions. This often leads to flux pockets and electric breakdown. If the initial seed field is too high, a higher initial velocity is required in order to compress the flux. This is because of the exponential increase in the magnetic force of the compressed volume. Additional to this is if the magnetic force becomes too large and the compression time is too long, conductor deformation can occur. If there is total destruction of the liner by the HE before the flux is compressed there is complete loss of all flux as well.

6 A NON-EXPLOSIVE TECHNIQUE

Current generators can produce large impulses but the generator requires a certain amount of HE. This requires specialised facilities and a large number of personel are required for the operation of such a device. This is often time consuming and limits the experimental time. Therefore the investigation into non-explosive methods was proposed. This provides a means for non-destructive experimental set-ups and the possibility for repeatability. The device could also be transported to any location and used for tests inside a Laboratory or at a remote location. A description of such a system is discussed below highlighting the advantages and disadvantages.

6.1 Mechanical system

The generator is divided into two sections, the mechanical system comprising of a two-stage light gas gun. The second section is the flux compression generator.

6.2 Two stage light-gas gun

A two stage light-gas gun is selected over a single stage gas gun as the projectile velocity is far higher. Helium is used in the compression chamber. The Helium as it is compressed experiences a temperature rise and this in turn increases its mach number. This prevents shock waves forming in front of the compressing piston as well as increases the projectile velocity. The projectile velocity is directly related to the speed of sound of the gas in the driving chamber [13]. The two-stage light gas as shown in *figure 6*, will comprise of a Reservoir which drives a piston and compresses the helium gas. A diaphragm at the end of the compression chamber bursts at a set pressure and this accelerates the projectile down the launch tube. The reservoir will be filled with compressed air. The projectile can be constructed of steel or aluminium. The required muzzle velocity from the gas gun is in the region of 1500 - 2000 m/s.

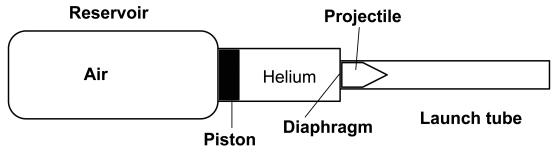


Figure 6. Schematic of a two-stage light gas gun

6.3 The flux compression chamber

The flux compression chamber is designed around the same principles as helical generators however with some design modifications that should eliminate some of the loss mechanisms therefore creating a more efficient device. This will also reduce the initial mechanical energy required for the compression volume. The stator coil is made of copper and is helical with an increasing coil pitch over the length of the generator. *Figure 7* shows the design of the liner, it must maintain its conductive path at all times however this design requires less initial kinetic energy to expand the liner as well as being reusable. The diagram of the liner shows a gap between the overlapped section, this is shown so the reader can see clearly how the liner is designed.

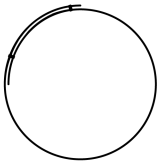


Figure 7. Liner design for the flux compression generator

The load and the liner will be electrically isolated and an external load is attached to the stator section. The expanding liner will only partially compress the initial volume. The reason for this will be explained in a later section. Attached to the outside of the helical coil is a movable bar that is electromagnetically controlled. As the projectile is moved through the volume of the generator the bar is pulled across the helical oil effectively shorting out the turns and therefore lowering the inductance of the coil which in turn increases the current in the system. *Figure 8* shows the compression chamber at the start of the flux compression process (a). the second diagram (b) shows a step during the compression process.

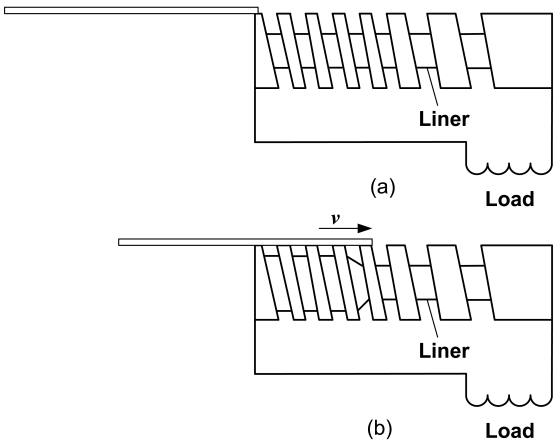


Figure 8. Daigrams showing the generator at t=0 (a), during the flux compression process (b)

6.4 Expected performances

The current delivered to the stator coil should be approximately 1 kA. The compression of the volume is approximately 50% of the original volume. The inductance for the orginal coil would be approximately 1.57 mH. Once the coils have been shorted the inductance of the stator would be aproximately 15.7 μH. This would indicate that in the ideal case the current gain would be 100. With the inclusion of the losses the output current gain would be approximately 15-20.

6.5 Advantages

The advantages of having the generator utilizing two different methods to increase the generator output aids in reducing the possibility of some of the losses occurring. Firstly the mechanical destruction of the generator does not occur as is the case in most other FCG designs. This allows for multiple experiments on the same device; the destruction of measurement systems is also avoided.

The liner will have a limited life span but it is reusable.

The probability of electric breakdown within the compression volume is drastically reduced. Electric breakdown in standard helical flux compression generators (HFCGs) packed with HE has a high probability of breakdown occurring as explained earlier. With this design the liner and stator do not come in contact and this therefore reduces the chances of electric breakdown losses. Magnetic forces are also kept at a lower level which reduces the initial mechanical energy required to compress the volume. The possibility of turn skipping (π-clocking) is also reduced as the liner and stator will not make contact.

Removing the HE from the generator volume allows the generator to be mobile and therefore experiments can be performed in any location.

6.6 Disadvantages

The disadvantages of such a design lies in the muzzle velocity of the projectile from the two-stage gas gun. The magnetic flux diffusion through the liner could be very high if the projectile velocity is too low causing the liner velocity to be very low. Erber and Latal [1] calculated the minimum velocity required for the compression of flux to be 300 m/s. The opposing forces due to the air and the mechanical frictional on the projectile trying to expand the liner could also reduce the liner velocity below this minimum, preventing flux compression from happening.

The shorting out of the stator coils by an external mechanism could have two major problems. If the shorting of the coils is not performed smoothly and quickly there is a chance that electric breakdown may occur between the bar and a turn of the coil. This is much like what would occur in an explosive generator. In this respect the output current would be dramatically reduced. The second problem with this mechanism is the time taken to short out the coils, if this is not in line with the expansion time of the liner then the output current will be less than the maximum possible current of the generator.

The system is not bound to a lab but there are areas that could cause problems with field work. The capacitor bank needs to be charged and this would be most easily performed by a generator. Therefore some mobile power source is required. The second is the method of filling the reservoir of the two-stage gas gun.

7 CONCLUSION

The development of flux compression generators has increased considerably over the last decade. Most generator designs are still based very closely on Sakharov's initial designs of the the MK-1 and MK-2 generators. Advancements in modern measuring techniques has increased the understanding of the process of flux compression and associated losses. Many more facilities around the world are now involved in the production of either high currents or high magnetic fields using flux compression techniques. The use of FCGs in industrial environments is also increasing with the application of FCGs in oil and mineral exploration as well as landmine detection.

The fundamental principles of flux compression rely primarily on the conservation of flux. Ignoring all losses this may be possible, however in real world application this is not the case and therefore in the design of generators it is important to be able to identify and reduce the losses of a generator. The design of this non-explosive generator is a method to try and reduce some of the losses by using alternate means of imitating the principles of flux compression. Partially compressing the volume reduces the risk of electric breakdown and the magnetic pressure is also reduced. An alternate means of reducing the inductance of the generator is therefore required. It should therefore be possible to design a non-explosive flux compression generator as long as the final liner velocity is maintained above 300 m/s.

8 ACKNOWLEDGEMENTS

The author would like to acknowledge Eskom for their support through TESP as well as DTI funding received through THRIP and NRF.

References

[1] T. Erber and H. G. Latal, "Flux compression theories," *Report on Progress in Physics*, vol. 33, pp. 1069–1127, 1970.

[2] H. Knoepfel, *Pulsed high magnetic fields*. North-Holland publishing Co, Amsterdam, 1970.

[3] A. Sakharov, *Collected scientifc works*. Marcel Dekker, Inc. New York, 1982.

[4] H. Knoepfel, *Magentic fields*. John Wiley & Sons, Inc. New York, 2000.

[5] I. Lindemuth, C. Ekdahl, C. Fowler, R. Reinovsky, S. Younger, V. Chernyshev, V. Mokhov, and A. Pavlovskii, "U.s./russian collaboration in high-energy-density hysics

using high explosive pulsed power: Ultrhigh current experiements, ultrahigh magnetic field applications, and progress toward controlled thermonuclear fusion," *IEEE transactions on plasma science*, vol. 25, no. 6, pp. 1357–1371, 1997.

[6] M. C. Enache, B. M. Novac, and I. R. Smith, "Three-dimensional modelling of helical flux-compression generators," *Digest of technical papers - IEEE international pulsed power conference*, pp. 253–255, 1999.

[7] B. Novac, I. Smith, M. Enache, and H. Stewardson, "Simple 2d model for helical flux-compression generators," *Laser and Particle beams*, vol. 15, no. 3, pp. 379–395, 1997.

[8] L. L. Altgilbers, M. Brown, I. Grishnaev, B. Novac, I. Smith, I. Tkach, and Y. Tkach, *Magnetocumulative Generators*. Springer-Verlag New York, 2000.

[9] T. Engel, W. Nunnally, and N. VanKirk, "Design and development of a noval flux compression generator for landmine detection applications," *IEEE transactions on Magnetics*, vol. 35, no. 1, pp. 245–249, 1999.

[10] M. Thompson, "Inductance calculation techniques - part ii: Approximations and handbook methods," *Power control and intelligent motion*, December 1999.

[11] G. R. Turner, "Inductance calculations for helical magnetocumulative generators,"

[12] E. Levi, Z. Zabar, and L. Birenbaum, "Basic performance of flux-xompression/expansion electromechanical converters," *IEEE transactions on plasma scence*, vol. 20, no. 5, pp. 554–561, 1992.

[13] C. Doolan, "A two-stage light gas gun for the study of high speed impact in propellants," tech. rep., Weapons systems division Aeronautical and Maritime research laboratory, 2001.

[14] A. Dickson and I. Jandrell, "Introduction to flux compression," *SAUPEC proceedings*, pp. 21–23, 2005.

9 LIST OF SYMBOLS

B_i	Initial flux density [T]
B_f	Final flux density [T]
A_i	Initial cross sectional area [m^2]
a_f	Final cross sectional area [m^2]
ϕ_i	Initial flux [Wb]
ϕ_f	Final flux [Wb]
L_i	Initial inductance [H]
L_f	Final inductance [H]
i_i	Initial current [A]
i_f	Final current [A]
U	Energy [J]
L	Inductance [H]
I	Current [A]
μ_0	Relative permeability of free space
H	Magnetic field strength [A/m]
R	Resistance [Ω]
m	Mass [kg]
v	Velocity [m/s]
ρ	Resistivity [Ω·m]
v_0	Initial velocity [m/s]
R_1	Initial position of conductor (radius 1) [m]
R_2	Final position of conductor (radius 2) [m]
μ	Relative permeability
L_0	Initial inductance [H]
I_0	Initial current [A]
a_i	Initial area [m^2]
a_f	Final area [m^2]
τ_0	Flux diffusion time constant (skin time)[s]
δ	Skin depth [m]
r	Thickness [m]
ω	Angular frequency [Hz]
σ	Conductivity [$(\Omega\cdot m)^{-1}$]
τ_s	Skin time [s]
E	Electromotive force [emf]

Introduction

Flux compression had its origin in military research laboratories during the end of the second world war. Flux compression relies heavily on magnetic theory, and this combined with some electric circuit theory is what Sakharov first used in suggesting high magnetic fields were possible from imploding metal liners. These ideas were developed into generators that could be used for current impulse generation as well. This development will be looked at from many different angles as the subject has grown over the last 50 years.

The fundamental physics of magnetic theory and electric theory is then presented. This provides a base for the understanding of flux compression systems. The ideal generator equations are then looked at and the same theory is applied to many different generator types. The fundamental principles however stay the same for all generator designs. An example based on Faradays law highlights some of the key areas important to a flux compression system.

Two generator models designed at Loughborough University, UK develop the flux compression theory further. These models highlight some of the more important loss components. The first model is a simple model which aided in the development of a 2D model. This comprehensive model breaks the generator down into discreet sections which can then be used for simulations over the entire operation time of the flux compression process.

The losses experienced in a flux compression generator can be severe. There are four main areas of losses and these are all discussed. In knowing what the losses of a generator can be, the designer can reduce areas that produce high losses. In some cases however a slight misalignment can have disastrous effects on the generators performance. Measurement devices can be used in current

generators to produce data so that the losses experienced can be better understood. These devices are however usually destroyed during each experiment therefore simple, low cost devices are often used. However they still provide sufficient information about the compression volume to aid in the development of new models.

With all the information provided a non-explosive flux compression generator was theoretically designed. This generator is designed with the intention of limiting many of the substantial losses and therefore allowing the initial kinetic energy required for the system to be less. Without the use of high explosives it makes the generator usable in many more locations. It also can be operated in confined spaces, increasing its potential for industrial applications.

Appendix A

A brief exploration into the history of flux compression is an important introduction to the subject. The initial physicists will be mentioned along with some of their contributions to the development of flux compression generators (FCGs). Modern day engineers and physicists will also be mentioned along with some of the application that FCGs have in modern society. A look into modern micro impulse components and generators will be presented. A final note about high temperature superconductors and flux compression will be made.

A.1 A history of flux compression

It is a debate as to who actually first came up with the concept of flux compression. This is due to the fact that initial research was performed behind closed door in military research laboratories. This prevented much of the earlier work being published. One of the fathers of of flux compression was Andrei D. Sakharov, a Russian physicist who formulated the concept of using high explosives to compress flux. The early work of Sakharov was eventually published in a collection of his scientific works in 1982 [1]. At the same time as Sakharov's initial work, M. Fowler in America was investigating similar principles. Fowler was not the first to do experiments on flux compression but his work on plate generators certainly went a long way in providing a launch pad for subsequent work to be performed in the States.

One of the most comprehensive open source papers published was written by T. Erber and H. G. Latal on flux compression theories [2]. The paper published in 1970 discusses some of the primary issues of flux compression theories and

provides the reader with some understanding of the principal equations for flux compression generators. At the same time in Europe H. Knoepfel published a book called "Pulsed high magnetic fields" [3]. The book explores all magnetic phenomenon describing a lot of the physics behind the different processes. This all leads into a couple of chapters on pulsed current generators, magnetic flux compression and ultra-high field generators. This book has subsequently been revised and relaunched in 2000 with the title of "Magnetic fields" [4].

Since the 1980's the development of magnetic flux compressors and high magnetic field generators has continually grown. International conferences have also started helping to develop a large pool of knowledge. There are many different laboratories and academic institutions these days that are conducting research on magnetic flux compression, a couple of these facilities are listed below.

In 1992 the governments of the United States and Russia encouraged lab-to-lab interactions [5]. This interaction occurred between the All-Russian Scientific Research Institute of Experimental Physics (VNIIEF) and the Los Alamos National Laboratory (LANL). The combined efforts have realised electrical currents ranging from 20 to 100 MA using magnetic flux compression generators. The work performed by the joint collaboration of these Institutes saw work in high magnetic fields and currents. One of Russia's designs for high magnetic currents was the Disk Explosive Magnetic Generator (DEMG). A 100 cm diameter DEMG has produced 100 MJ at 256 MA [5]. The generator is a modular design and therefore there is a possibility to stack numerous stages and therefore produce a 1 GJ generator.
The following list is of flux compression test facilities from around the world.

- High stationary magnetic fields laboratory – Russia
- Kurchatov institute – Russia
- High field laboratory for superconducting materials – Japan
- Tsubuka magnet laboratory – China
- International laboratory of high magnetic fields and low temperatures – Poland
- Grenoble high magnetic field laboratory – France

- National high magnetic field laboratory – USA
- Los Alamos National laboratory – USA
- Loughborough University – UK

Present day pioneers are Neuber and Dickens from the USA and Novac, Smith and Knoepfel from the UK and Europe. The researchers above demonstrate the bulk of the work being produced as well as providing a wealth of knowledge which many researchers now draw from. There are many researchers in the the area of flux compression but most work is based on that produced by one of the above researchers. There are some real world applications for Flux compression generators but most systems are still used within laboratories for the analysis of the physical properties of matter exposed to high magnetic fields. Interesting present day work that is being performed is from the University of Missouri - Columbia where they are looking into flux compression projectiles for the detection of land mines [6].

A.1.1 Typical areas of use

The following lists are past and current areas that flux compression generators are used for [7, 8].
Historical uses:

- Charged particle beam diodes
- Imploding plasmas
- Large collection of defence related applications

Modern day uses:

- Biological samples
  - Water from municipal drinking supplies
  - Effluents from combustion processes

- Environmental
- Biomedical
- Hydrodynamics programs and high magnetic field research
- Exploration for oil and minerals
- Landmine detection

Material science under high magnetic fields

In the case of high magnetic fields greater then 1 T and temperatures in the region of 1K phenomena in condensed matter physics has been observed. These include items such as fractional quantum hall effect, composite fermion behaviour in epitaxial semiconductors and new density wave states for spin and charge in organic conductors [9]. As the higher magnetic fields are being produced, physicists are able to study all electrons in the lowest Landau level, pushing the previous levels of understanding in material sciences.

Landmine detection

The work done in Missouri regarding the landmine detection is of some interest to the work being investigated here. Though the applications are different the initial Kinetic energy of the mechanical system is very similar. A brief description of the work undertaken at University of Missouri will be discussed.

Their system is called the AKEM (Aero-kinetic-Electro-Magnetic)[10], which converts kinetic energy into electrical energy. The projectile detonates on impact sending a radar wave propagating through the soil. If the propagated wave comes into contact with any land mines a footprint of the object is seen on a sensor screens. Two projectile types were investigated, the first being a magnetic flux compression projectile and the second being a piezoelectric projectile.

An illustration of the magnetic flux compression generator can be seen in *figure A.1.* The projectile needs some form of seed current injected into its

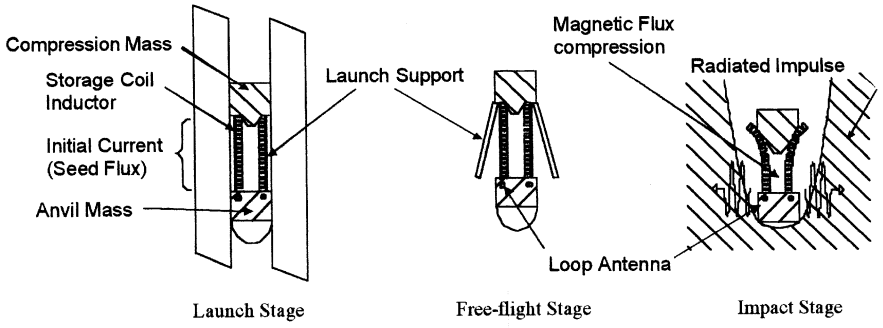


Figure A.1: Operation of the AKEM magnetic flux compression projectile [6].

volume prior to launching. On impact with the ground the compression mass moves through the storage coil and compresses the flux. This increases the electrical energy of the system which then produces a radar wave which propagates through the soil.

The laboratory set-up for the experiment consisted of a scaled projectile being launched by a light-gas gun into a clay target. A Chronograph is used to measure the speed of the projectile. The approximate pressure used was 34.5 MPa (5000 psi), which could produce a projectile speed of approximately 1000 m/s [6]. With their work they modelled an ideal gas gun but included gas inertial effects. The expression used for the time dependant gas pressure, $p(t)$, at the projectile base is given by [6]:

$$p(t) = p_0 \left[1 - \frac{u(t)}{\frac{2}{\gamma-1} a_0} \right]^{\frac{2\gamma}{\gamma-1}} \tag{A.1.1}$$

where:

- $u(t)$ is the projectile's velocity as a function of time
- p_0 is the initial helium pressure
- a_0 is the initial speed of sound in the pressurised helium
- γ is the ratio of specific heats for helium

Using PSpice they were able to model the gas gun and projectile up to and including the impact of the projectile. Their simulated and experimental results were in agreement and the system was able to increase the current from 150 to 468 mA.

A.2 Modern pulsed power

Pulsed power refers to the technology of accumulating energy over a relatively long period of time, then compressing it in a relatively short period to deliver very large power pulses to a load [8, 11]. There is a constant need for better performance, more compact design and higher energy outputs. This has spurred on the development of pulsed power devices. A lot of everyday applications, particularly in the medical and environmental fields use pulsed power devices. There is a grey area between the definition of compact and ultracompact pulsed power as they basically deal with the same idea. However the ultracompact system often uses modern advances in device technology to create extremely small devices. As an example of this, a 750 kV Cockcroft-Walton voltage multiplier that is used at Los Alamos Neutron Science Center to accelerate a hydrogen ion beam for injection into an RF linear accelerator, occupies a large room. In comparison to this a surface mount Cockcroft-Walton multiplier is only 18.5 mm in length by 8.9 mm wide and produces 3 kV [12].

Some fundamental work has gone into designing faster switches and better and faster capacitors. These all aid in producing larger and faster impulses. There are of course still limits to the advances in the technology. Prime power is one of the areas that is still behind the times. Advances in areas such as turboalternators, microfuel cells and microsized internal combustion engines are helping to improve this area. Case Western Reserve University in Cleveland, Ohio, is working on a fuel cell on a 2×2 cm square of silicon that will generate ten times more power and have two orders of magnitude more energy then present day state-of-the-art thin-film batteries [12]. One of the issues facing these modern micro power sources is the removal of heat from the devices. Advances in thermoelectric converters is aiding in removing the heat but also efficiently converting this heat back into electricity.

A.2.1 Flux compression with high temperature superconductors

In the early 1990s a group did some research into the effectiveness of high temperature superconductors (HTS) for a flux compression system [13]. The work

is actually aimed at producing a magnet with a large variation of field strength from 6 T down to 0.05 T. It is required that a magnet cycle between these values as it was to be used in a refrigeration unit for the cooling of infrared detectors in space.
The apparatus used in the exploration of the generation HTS magnets is a block with two holes and a plunger. The holes are 0.95 cm and 0.52 cm with the plunger being 0.93 cm. As the plunger is pushed into the bigger hole the flux is forced into the smaller hole where a hall probe measures the field. Some flux does penetrate the plunger so the field is not exactly proportional to the ratio of the hole sizes. In order to create a high field permanent magnet the plunger was then removed, a field again being applied to the block and then the permanent magnet is once more inserted into the block, increasing the flux compression. This process is continued until the flux penetrates through the walls of the block and further flux compression is not possible.

A.3 Summary

There have been many prominent flux compression researchers mentioned above. They have all contributed in some manner to the general knowledge of the subject. Two groups in particular stand out, Erber and Latal for providing the first comprehensive open source paper in 1970, that covers the majority of the theory related to flux compression. The second is Novac and Smith who are two of the top modern researchers of flux compression. From their contributions this area of research has grown incredibly. There are test laboratories all over the world now, performing research into FCGs. New modern day applications are being found for FCGs in particular in the use of landmine detection. The next section will explore the physics of how and why a flux compression generator works.

Appendix B

From the previous section the history of flux compressors was explored, giving the origins of flux compressors and the present day test facilities involved in the production of either high magnetic fields or current impulses. The physics behind the process is very important for the understanding of FCGs. The different physical processes will be presented including some of the necessary electrical theory. Some basic theory used in gas gun design will also be discussed.

B.1 Physical processes and definitions

This section aims at highlighting the key points behind the physical processes involved in flux compression. Without an understanding of some of the basic physical principles a full understanding for the events that take place in a flux compressor are not totally appreciated. The physical equations will be highlighted with key aspects being defined.

B.1.1 Magnetic flux

There are two routes that can be taken in solving the problem of flux compression. The first is using Faraday's law of induction and Lenz's law. The second method is by Maxwell's equations. Faraday found that moving a magnet through a conducting coil will induce a current in the coil, which in turn induces an emf. He further went on to establish the fact that the emf was not necessarily related to the change of the magnetic field, but it was in fact proportional to the rate of change of the magnetic flux (Φ_B)[14]. The magnetic

flux is defined by:

$$\Phi_B = \int \mathbf{B} \cdot dA \tag{B.1.1}$$

The unit of magnetic flux is the tesla· meter ^{2} which is also referred to as the weber [Wb]. The magnetic field $\mathbf{B}$ is usually referred to as the magnetic flux density and is equal to the flux per unit area (Φ_B/A). From Faraday's investigation he produced the result of:

$$\mathscr{E} = -\frac{d\Phi_B}{dt} \tag{B.1.2}$$

which states that the induced emf in a circuit is equal to the rate of change of the magnetic flux through it [14]. This is Faraday's law of induction and a fundamental relation in electromagnetism. If a circuit contains N closely wrapped loops, then Faraday's law can be expanded to:

$$\mathscr{E} = -N\frac{d\Phi_B}{dt} \tag{B.1.3}$$

The minus sign gives the direction of movement and further goes on to describe Lenz's law which states:

> An induced emf always gives rise to a current whose magnetic field opposes the original change of magnetic flux.

Faraday's law can be applied to moving bodies as that shown in *figure B.1.* In this case Faraday's law can be modified as follows to provide a result for the moving conductor.

$$\mathscr{E} = \frac{d\Phi}{dt} = \frac{\mathbf{B}dA}{dt} = \frac{\mathbf{B}lvdt}{dt} = \mathbf{B}lv \tag{B.1.4}$$

For this equation to hold all components, B, l and v must be perpendicular to each other.

A changing magnetic field produces an electric field

When a current flows through a conductor there is an electric field which causes the electrons to attain a drift velocity v_d. As there is a induced current in the conductor in *figure B.1*, there must be an electric field in the conductor. This

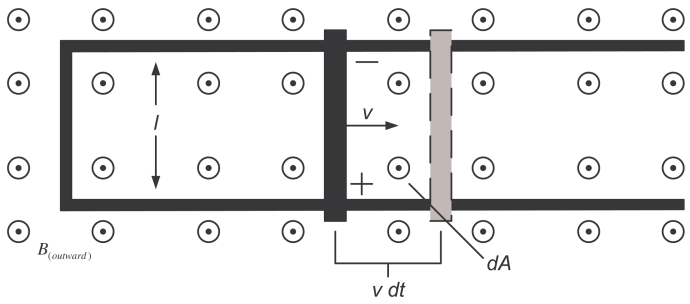


Figure B.1: A conducting rod moving on a U-shaped conductor in a uniform magnetic field [14].

electric field is equal to the force per unit charge, $\mathbf{E} = F/q$ and the force is equal to $F = qv\mathbf{B}$ which therefore produces:

$$E = \frac{qv\mathbf{B}}{q} = v\mathbf{B} \tag{B.1.5}$$

This equation can be generalised to non perpendicular environments and results in:

$$\mathbf{E} = v \times \mathbf{B} \tag{B.1.6}$$

If the original idea is investigated in the same way, a moving conductor is not producing the electric field but a changing magnetic field. Therefore a magnetic field must produce an electric field, which according to Giancoli [14] is true regardless of any region in space and the need for conductors or wires to be present. Thus the following mathematical equation was produced to describe the relation between the electric field and potential difference between any two points in space.

$$V_{ab} = \int_a^b \mathbf{E} \cdot dl \tag{B.1.7}$$

The emf $\mathscr{E}$ induced in a circuit is equal to the work done per unit charge by the electric field, which equals the integral of $\mathbf{E} \cdot dl$ around the closed path.

$$\mathscr{E} = \oint \mathbf{E} \cdot dl \tag{B.1.8}$$

This can be combined with Faraday's law to obtain

$$\oint \mathbf{E} \cdot dl = -\frac{d\Phi_B}{dt} \tag{B.1.9}$$

which relates the changing magnetic field to the electric field it produces. The integral on the left is taken around the path enclosing the area through which

the magnetic flux is changing. This is valid for any region of space. In the case of electrostatics the potential difference round a closed loop equates to zero. An electrostatic force is a conservative force, therefore a potential energy can be defined. However when an electric field is produced by a magnetic field the integral around a closed path is not zero, given in *equation B.1.9*. Therefore the forces due to a changing magnetic field are non-conservative and this in turn means the electric field produced by a changing magnetic field is a non-conservative field.

Magnetic fields produced from a solenoid

From Ampère's law it is possible to calculate the magnetic field inside a solenoid. The result is

$$\mathbf{B} = \mu_0 n I \tag{B.1.10}$$

where $n = N/l$ which is the number of loops per unit length.

B.1.2 Energy stored in a magnetic field

The energy stored in an inductor is related to the current flowing through the coil. This energy is equal to the work done in producing a particular current in an inductor. The work is defined as

$$W = \int dW = \int_0^I LI dI = \frac{1}{2} L I^2 = U. \tag{B.1.11}$$

The work is defined by W and the energy is defined by U. For the purpose of this work and for reasons of comparison the energy stored within a capacitor is defined by:

$$U = \frac{1}{2} C V^2 \tag{B.1.12}$$

If the original equation for the energy stored in an inductor is manipulated the energy stored in an inductor can also be calculated using the magnetic flux density and the area enclosed by a solenoid, which is defined by:

$$U = \frac{1}{2} \frac{\mathbf{B}^2}{\mu_0} A l \tag{B.1.13}$$

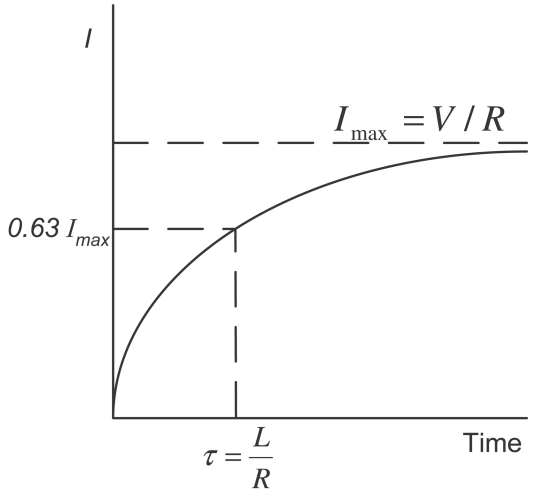


Figure B.2: The current rise within a conductor.

B.1.3 LR Circuit

For flux compression to have the most efficient results it is important that the detonation in the case of an explosive HFG is initiated at the time when the current in the coil is a maximum, therefore producing a maximum magnetic field. An inductor will have some internal resistance and this is why an inductor is modelled as an inductor and resistor in series. When a source is attached across an inductor the current begins to flow. The induced emf in the inductor opposes the current flow. The current flowing in the circuit also travels through the resistor which reduces the emf across the inductor lowering its impedance and therefore the current rises slowly as shown in *figure B.2*. The equation that describes this rise is defined as:

$$I = \frac{V}{L}\left(1 - e^{\frac{-t}{\tau}}\right) \tag{B.1.14}$$

For the equation $\tau = L/R$ which is the time constant for the system and describes the time required for the current to reach 63% of its maximum value.

B.2 Inductance

Magnetic flux compression is based fundamentally around the current and inductance of the system. It is therefore essential to have a comprehensive understanding of the inductance of a system as well as methods for calculating

the values of system. This section defines inductance, and provides various methods for calculating the inductance for different systems. Emphasis is made on the research being undertaken here.

Inductance is defined as the flux linkage per ampere [15]. Depending on the generator design the inductance to be calculated varies. Therefore both the self and mutual inductances will be defined in this section.

B.3 Self – Inductance

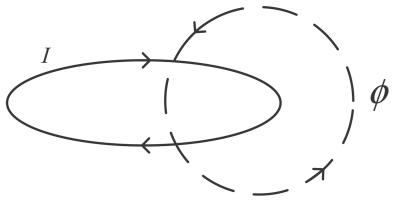


Figure B.3: The flux linkage of a single turn current carrying coil.

To better understand inductance the concept of flux linkage will first be introduced. In *figure B.3* a current carrying coil is linked via a flux line. In the case of a multi turn coil, if the flux produced by these turns links all the turns, then the flux linkage can be defined as:

$$\lambda = N\phi \qquad W.turns \tag{B.3.1}$$

Where N is the number of turns being linked by the flux ϕ. Therefore in the case where only one coil is present there is a linking of the flux among the coils from the induced changing current in its own coils. The inductance of such a system in relation to its flux linkage is therefore:

$$L = \frac{\lambda}{i} \tag{B.3.2}$$

This in turn, due to the definition of flux linkage, makes the inductance equal to:

$$L = \frac{N\phi}{I} \tag{B.3.3}$$

From Faraday's law the emf $\mathscr{E}$ induced in a coil of inductance L is:

$$\mathscr{E} = -N\frac{d\Phi}{dt} = -L\frac{dI}{dt} \tag{B.3.4}$$

B.3.1 Finite-length solenoid

There are many different formulas available for this calculation. The following was taken from all the different methods presented by Turner, Novac and Knoepfel as it is the simplest and in a lot of cases it is what the other equations resolve to:

$$L \approx \frac{10\pi\mu_0 N^2 a^2}{9a + 10l} \tag{B.3.5}$$

In the case where the length of the coil l is larger then $0.8a$ then the accuracy is often better the 1%. In this equation:

- N is the number of turns of the coil
- a is the radius of the solenoid
- l is the length of the solenoid

If there is a need for calculating the inductances of very short coils with large diameters there are equations available for this. For this work it is not required and therefore will not be defined.

B.4 Mutual – Inductance

Depending on the design of a generator the mutual inductance of the system will have to be found. Many different ways are available for this however in this section only two will be considered. The first is that proposed by Maxwell, using standard elliptic integrals $K(k)$ and $E(k)$. The equation is defined as [16]:

$$M_{12} = \mu_0\sqrt{a_1 a_2}\frac{2}{k}\left[\left(1 - \frac{k^2}{2}\right)K(k) - E(k)\right] \tag{B.4.1}$$

where

$$k = \sqrt{\frac{4a_1 a_2}{(a_1 + a_2)^2 + h^2}} \tag{B.4.2}$$

Figure B.4 shows the relationship of the different components for the mutual inductance equations. The second method was proposed by Geoffrey Turner of the National Energy Council of South Africa (NECSA). From the original idea

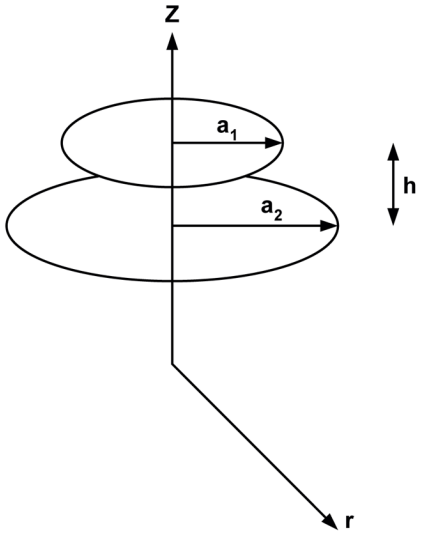


Figure B.4: The mutual inductance between two loops.

used above Turner proposed using the complete Legendre elliptic integral of the first kind $F(\phi, k)$ and a linear combination of the Legendre elliptic integrals of the first and second kind $D(\phi, k)$[17]. Turner's paper describes the method in obtaining the mutual inductance between two coils. The resulting equation is:

$$M_{ij} = \frac{2\mu_0 r_i r_j}{\sqrt{d_{ij}^2 + \left(r - i - r_j\right)^2}} \times \left(F\left(\frac{\pi}{2}, k\right) - 2D\left(\frac{\pi}{2}, k\right)\right) \tag{B.4.3}$$

The value of the self inductance using *equation B.4.3* is calculated from:

$$L = \sum_{i=1}^{i=N} \sum_{j=1}^{j=N} M_{ij} \tag{B.4.4}$$

For most generators mutual inductance plays a small part, and at times can be regarded as a constant even as the liner expands outwards towards the stator. Novac *et al* found that there were slight discontinuities from doing this but an error of less then 5% was still recorded [18].

B.5 Mechanical characteristics

B.5.1 Characteristic gas equations

Pressure is the normal force per unit area. The general units used for pressure are N/m^2. It is important to introduce two components for the analysis of gases in a volume. The first is the perfect gas equation of state, which is derived from the the kinetic theory and neglects molecular volume and inter-molecular forces [19]. The perfect gas equation therefore only holds under conditions of relatively low pressure and/or high temperatures. The equations is defined as:

$$p = \rho RT \tag{B.5.1}$$

Where:

- p is the absolute pressure $[N/m^2]$
- ρ is the density $[kg/m^3]$
- T is the absolute temperature [K]
- R is the individual gas constant $\left[\frac{N-m}{kg-K}\right]$

For the SI unit system the individual gas constant is approximated by dividing 8314 by the molecular weight. Therefore R for air is equal to approximately 287 $\frac{N-m}{kg-K}$.

The second formula is used to understand the flow of air within a chamber or pipe. The mass flow rate is introduced and is defined by:

$$\dot{m} = \rho AV \tag{B.5.2}$$

where:

- $\dot{m}$ is the mass flow rate
- A is the cross sectional area
- V is the average velocity ($U_m/2$)

B.5.2 Projectile energy

Using Newton's second law of motion we can describe the initial acceleration of a projectile from a gas gun.

$$a = \frac{F}{m} \tag{B.5.3}$$

Since the projectile will be coming into contact with a metal cylinder there will be a retarding friction between the two objects. In this case the original force calculated from the system needs to be multiplied by the coefficient of kinetic friction (μ_k). From Giancoli [14] the following values will be useful to this work: The kinetic energy of a moving body is described by:

Surface	**Coefficient of kinetic friction μ_k**
Metal on Metal (lubricated)	0.07
Steel on steel (unlubricated)	0.6

Table B.1: Coefficients of kinetic friction for metals.

$$KE = \frac{1}{2}mv^2 \tag{B.5.4}$$

which if a particle is moved form rest this kinetic energy (KE) value is also equal to the work done, $W = \Delta KE$.

B.5.3 Projectile velocity

The velocity of the liner is very important to the flux compression process. It is therefore essential that sufficient mechanical energy is available for the compression of the flux. Not using explosives therefore requires another means of obtaining sufficient energy for the process. Sufficient energy has been obtained from using gas guns. In most cases these have been two stage devices as the force and therefore final velocity obtained is higher. Assuming a constant applied force on a projectile as the gas expands the following equations of motion can be used.

$$mv = tF \quad , \quad \frac{1}{2}mv^2 = lF \tag{B.5.5}$$

The second equation describes the final energy of a projectile due to a constant force over a finite length and therefore the final muzzle velocity can be solved

for. However in real world application as soon as the projectile starts to move there is a decrease of the applied force. Taking this change of pressure into account the equation defining this lower muzzle velocity of the projectile is defined by:

$$v_{exp} = \left(\frac{2}{\gamma - 1}\right) a_0 \; = \frac{1}{\gamma - 1}\sqrt{\frac{\gamma R T_0}{M}} \tag{B.5.6}$$

where:

- T_0 is the initial temperature of the driving gas in kelvin
- γ is the adiabatic factor, the ratio of specific heat capacities at constant pressure and constant volume (C_p/C_v)
- R is the universal gas constant
- M is the molecular weight of the driving gas

What has been found is that the velocity of the projectile is dependent on the speed of sound a_0, of the driving gas [20]. Therefore most high velocity gas gun systems use a two stage light-gas gun using nitrogen or helium as the projectile driving gas [6, 20]. Velocities in the order of 2000 m/s have been obtained [21]. Another method that can be used to determine the muzzle velocity of the projectile from the two stage light-gas gun is by the pressure produced behind the projectile. This pressure as has been mentioned above will become smaller as the projectile moves down the length of the launch tube. The following equation describes this change of pressure:

$$p(t) = P_o \left[1 - \frac{u(t)}{\frac{2}{\gamma-1} a_o}\right]^{\frac{2\gamma}{\gamma-1}} \tag{B.5.7}$$

Where:

- $u(t)$ is the projectile's velocity as a function of time
- p_o is the initial helium pressure

This equation is based on the ideal gun model but does include gas inertial effects [6].

B.6 Summary

The physics behind flux compression has been explained. This section did not illustrate or deal with flux compression in any form; this will be covered in the next section. The tools needed to understand the fundamentals of flux compression were covered. Particular emphasis was placed on magnetic theory and its interaction with conductors. Electrical theory in the form of inductance was covered as both the magnetic and electrical components rely heavily on this phenomenon. The energy stored in a magnetic field was also briefly touched on. The fundamental properties for the operation of a two-stage light gas gun were also covered. This will aid in the design of such a device for the process of using it in a flux compression generator design. Having understood some of the physics the fundamental principles of flux compression will be explored in the next appendix. The main generator types will be discussed with particular emphasis on current generators.

Appendix C

The fundamental theory about the physics and electrical principles were discussed in the previous section. This section will combine this theory presenting both ideal and real world cases. Generators for producing high magnetic fields and current impulses will be discussed, providing theory for both types of generator design. Some examples are given to best highlight important issues within an FCG.

C.1 Flux

C.1.1 What is Flux?

There are two types of flux that are considered, they are magnetic and electric flux. This work deals with magnetic flux and therefore unless otherwise stated, flux refers to magnetic flux.

So what is flux? Magnetic flux is a collection of a number of lines of magnetic intensity. Magnetic intensity is a collection of lines of force crossing a square centimetre area. Where the area and the lines of force are perpendicular to each other. Lines of force are representative of the magnetic field existing in the neighbourhood of a magnetic pole. Therefore stated again, what is flux? It is the number of magnetic lines, represented as lines of force that are present in a square centimetre. The number of lines represents the intensity of the field and this is called magnetic flux.

C.1.2 Energy available in flux compression – energy in a magnetic field

In most cases the energy in a magnetic field is calculated from the initial energy used to create the magnetic field. This equations is stated as:

$$U = \frac{1}{2}LI^2 \tag{C.1.1}$$

It is also known that:

$$L = \frac{N\phi}{I} \tag{C.1.2}$$

Therefore, the energy equation can be rewritten as:

$$U = \frac{1}{2}N\phi I = \frac{1}{2}\frac{\mu_0 N^2 A}{l} \tag{C.1.3}$$

In most cases this shows that if the energy is conserved then the energy that is initially in the field must be available in other forms. From Sakharov's earlier work on magnetic flux compression, he defined the energy of the magnetic field to be [1]:

$$W = \left(\frac{\mathbf{H}^2}{8\pi}\right)\pi R^2 l \tag{C.1.4}$$

C.2 The Ideal Flux compressor – some basic theory

The ideal case of flux compression can best be described as follows:

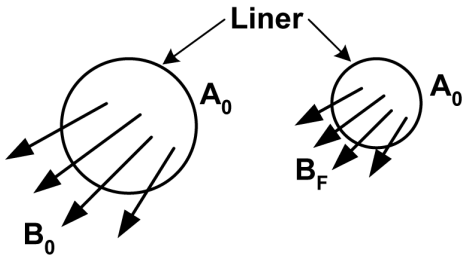


Figure C.1: Field conservation by varying a conductors area [5].

An area with initial magnetic field of $\mathbf{B}_0$ and area A_0 is shown in *figure C.1*, if the area is made smaller A_f the final flux $\mathbf{B}_f$ must increase as Faraday's law requires the magnetic flux must be conserved [5].

$$\mathbf{B}_F A_F = \mathbf{B}_0 A_0 \tag{C.2.1}$$

$$\phi_f = \phi_0 \tag{C.2.2}$$

If a conductor has zero resistivity the induced surface currents would prevent flux from penetrating into the conductor. This would result in a field increasing at $1/r$ for a plane conductor system and $1/r^2$ for an imploding cylinder [22].

This can be extended to the current and inductance of a circuit. The flux produced by an electric circuit is equal to the current (I) times the inductance (L). therefore the relationship of the flux represented in *equation C.2.2* can be rewritten as:

$$L_i I_i = L_f I_f \tag{C.2.3}$$

All these relationships, though being for ideal cases show that depending on the required output from a generator, a fundamental relationship exists. The generator being designed in this work is looking at impulse generation and therefore the relationship shown in *equation C.2.3* is of greatest importance. The current gain of an ideal system would be:

$$I_f = I_i \frac{L_i}{L_f} \tag{C.2.4}$$

Of course there will always be losses in a real world system and therefore it is relevant to introduce a factor β to account for system losses. The current gain is therefore described as [7]:

$$G_I = \frac{I_f}{I_i} = \left(\frac{L_i}{L_f}\right)^{\beta} \tag{C.2.5}$$

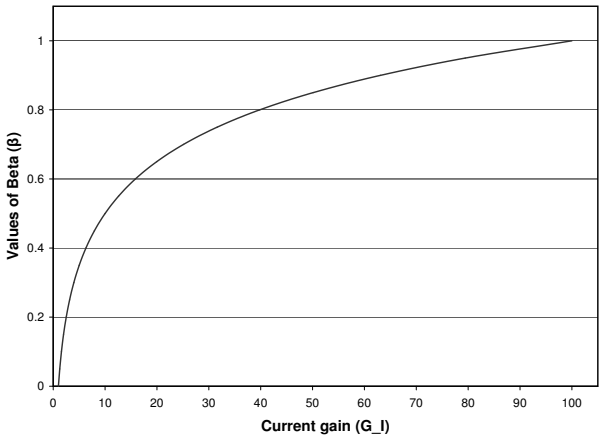


Figure C.2: Graph showing the relationship of β to the current gain (G_I) of a flux compression generator.

For an ideal case β will be equal to 1; for most helical flux compression generators the values of β are between 0.6 - 0.8 [7]. *Figure C.2* shows the relationship of the current gain to the value of β. Obviously the higher β is the greater the gain; however once the value of β falls below 0.5 current gain still occurs but there will be a loss of energy of the system. The methods of attaining the highest gain for both energy and current is by making the L_f as small as possible and the β factor as close to 1 as possible.

C.3 Equivalent circuit for current generators

A circuit describing the fundamental operation of a flux compression generator can be found in most of the modern books written on the subject [4, 23]. There are slight variations in the subscripts within these texts so the methods followed by Knoepfel will be used. *Figure C.3* shows the equivalent circuit for a generator, the dotted section at the bottom of the figure is the seed current branch.
There is a total time-dependent inductance in the circuit which is defined as:

$$L(t) = L_C(t) + L_L \tag{C.3.1}$$

Where:

- $L_C(t)$ is the compression inductance
- L_L is the load inductance

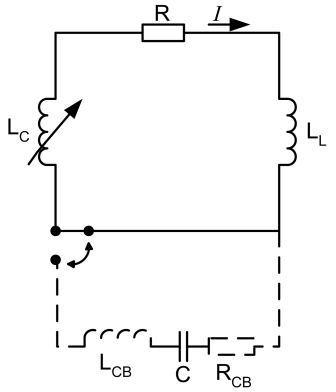


Figure C.3: Equivalent circuit diagram of a flux compression generator [4].

The resistance R which is time dependent is a representation of the magnetic flux losses. The differential equation defines the circuit:

$$\frac{d(LI)}{dt} + RI = 0 \tag{C.3.2}$$

Solving the differential equation for any instant in time produces:

$$LI = L_0 I_0 \exp\left\{ -\int_0^t \frac{R}{L} dt \right\} \tag{C.3.3}$$

where:

- $L_0 = L_{Co} + L_L$ is the total inductance at time equal to zero
- I_0 is the initial current obtained from the capacitor bank shown at the bottom of *figure C.3*

The flux coefficient is defined by:

$$\lambda(t) = \frac{LI}{L_0 I_0} = \exp\left\{ -\int_0^t \frac{R}{L} dt \right\} \tag{C.3.4}$$

and the inductance coefficient or inductive compression ratio is defined by:

$$\gamma_L(t) = \frac{L_0}{L} \tag{C.3.5}$$

The current gain coefficient or current multiplication ratio is defined by:

$$\gamma_I(t) = \frac{I}{I_0} = \frac{\mathbf{H}}{\mathbf{H}_0} \tag{C.3.6}$$

This holds as magnetic fields are proportional to the current and therefore the *equation C.3.3* can be written as:

$$\frac{I(t)}{I_0} = \gamma_I(t) = \gamma_L(t)\lambda_k(t) \tag{C.3.7}$$

Multiplying *equation C.3.2* by I the energy of the system is defined by:

$$-\frac{1}{2} I^2 \frac{dL}{dt} = RI^2 + \frac{d}{dt}\left[\frac{1}{2} LI^2\right] \tag{C.3.8}$$

Integrating this equation the potential magnetic energy of the circuit is:

$$\frac{W(t)}{W_{Mo}} = \frac{LI^2}{L_0 I_0^2} \tag{C.3.9}$$

where

$$W_{Mo} = \frac{1}{2} I_0^2 L_0 \tag{C.3.10}$$

is the initial energy of the generator.

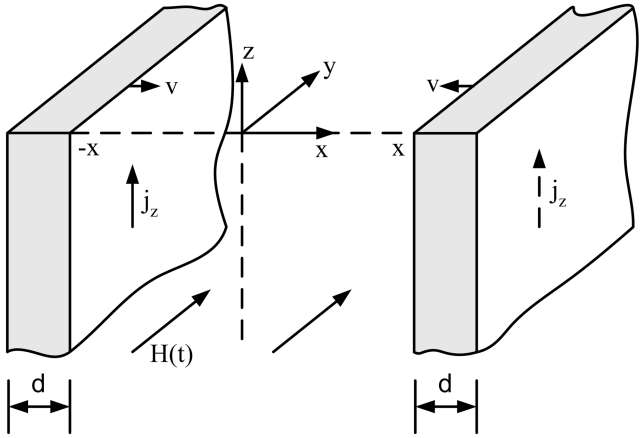


Figure C.4: Parallel plane compression system [4].

C.3.1 Flux compression by incompressible plane conductors

The system shown in *figure C.4* is that of two infinitely large conducting planes moving toward each other with a velocity of v. There is perfect symmetry; therefore the system could be seen as a piston and a stationary wall. The initial kinetic energy of one of the walls is:

$$W_{Ko} = \frac{1}{2}\rho d v_0^2 \tag{C.3.11}$$

Where d is the wall thickness and ρ is the density of the material. The initial magnetic energy in the volume between the two planes is:

$$M_{Mo} = \frac{1}{2}\mu_0 \mathbf{H}_0^2 x_0 \tag{C.3.12}$$

Where $\mathbf{H}_0$ is the field within the volume between the two planes and x_0 is the volume between the planes. Assuming the two planes are made of an ideal conductor ($\sigma \to \infty$) then:

$$\mu_0 \mathbf{H} x = \mu_0 \mathbf{H}_0 x_0 \tag{C.3.13}$$

$$\tfrac{1}{2}\mu_0 \mathbf{H}^2 x + \tfrac{1}{2}\rho d v^2 = W_{Mo} + W_{Ko} \tag{C.3.14}$$

From these equations it is possible to calculate the velocity of the moving plane by differentiating *equation C.3.13*. As the plane approaches the stationary plane the magnetic pressure grows and eventually will bring the moving plane to rest, this is termed the turnaround point. At this stage the Kinetic energy

has all been converted into magnetic energy and is defined by:

$$\frac{\mathbf{H}_t}{\mathbf{H}_0} = \frac{x_0}{x_t} = 1 + \frac{W_{Ko}}{W_{Mo}} \tag{C.3.15}$$

From this equation it is possible to see that a weaker initial field can help in generating a larger field at the turn around point up to some finite level. This is due to the fact that the conductivity is not infinite and therefore there will be flux penetration into the liner.

The skin depth is defined by s_ϕ and is the depth the flux will penetrate into a conductor. The skin depth is defined by:

$$s_\phi = \sqrt{\kappa_0 \tau} \tag{C.3.16}$$

Where τ is the diffusivity time and κ_0 is the magnetic diffusivity which is defined by:

$$\kappa = \frac{1}{\sigma \mu} \tag{C.3.17}$$

Another term that must be introduced at this stage is the magnetic Reynolds number which is:

$$R_m = \frac{x_0 v_0}{\kappa_0} \tag{C.3.18}$$

The magnetic Reynolds number represents the ratio of the diffusion decay-time over the compression time [4]. It can be seen from this that a large Reynolds number means the diffusion losses are not important. Combining the initial circuit equations and the diffusion characteristics of the plane conductors the field amplification for the two planes is:

$$\frac{\mathbf{H}}{\mathbf{H}_0} \approx \frac{l_0}{l} \exp\left[\frac{2}{\sqrt{R_m}}\left(1 - \sqrt{\frac{l_0}{l}}\right)\right] \tag{C.3.19}$$

If the conductor is able to reach a position where $x \to 0$ a maximum field amplification is possible which is defined by:

$$\frac{\mathbf{H}_m}{\mathbf{H}_0} \approx \frac{R_m}{e^2} + \frac{\sqrt{R_m}}{e^2} \tag{C.3.20}$$

C.4 Magnetic flux compression by a rod and rail system

From the section on the physics relating to flux compression, Faraday's law of induction was introduced. Namias [24] uses this law in conjunction with a rod

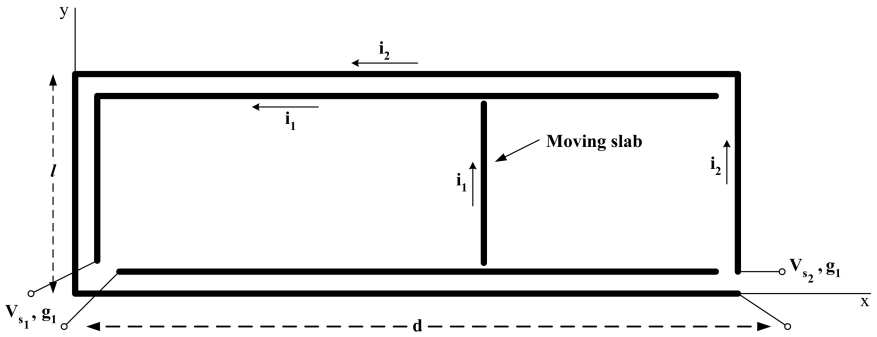


Figure C.5: Rod and rails system used in Namias's work [24].

and rail system to demonstrate flux compression. Using the rod and rails he demonstrates different parameters that will have an influence on the output. One such parameter is the source of the movement of the rod; it can either have a constant applied force or be moving with a constant velocity. Another case is the introduction of a constant field produced from an external source. A couple of questions are raised with such a system and they are [24]:

1. Is the motional emf given by $\mathbf{B}lv$, where $\mathbf{B} = \mathbf{B}_{applied} + \mathbf{B}_{induced}$?
2. How is the variation in time of $B_{induced}$ taken into account?
3. How is the self-inductive effect properly introduced since the coefficient of self-inductance varies with time?
4. How is the magnetic force on the rod calculated to include the effect of the induced field?
5. What role does $\mathbf{B}_{induced}$ play in the the energy balance and is the stored energy still given by the familiar expression $\frac{1}{2}Li^2$?
6. How is the electromechanical energy transfer calculated when induced effects are taken into account?

In his analysis of the rod and rails system Namias explores both the mechanical and electrical components separately. *Figure C.5* shows both examples of Namias's rod and rail system. For his initial example the outer rail is not used, only when he investigates the effect of the source of $\mathbf{B}_a$ is it used. Investigation

into an initial rod and rail system produces the following equations representing the electromechanical system:

$$V_s = \mathbf{B}_a lv + \mu_0 ilv + \mu_0 lx\frac{di}{dt} + \frac{i}{g} + \frac{d\mathbf{B}_a}{dt}lx \tag{C.4.1}$$

$$m\frac{dv}{dt} = F_s + il\mathbf{B}_a + \frac{1}{2}i^2\mu_o l \tag{C.4.2}$$

Where:

- $\mathbf{B}_a$ is the applied uniform field
- l is width separating the rails
- x is the distance the rod is away from the end of the closed "U"
- g is the total conductance of the system
- v is the velocity of the rod
- m is the mass per unit length of the moving rod
- F_s is the applied force to the rod
- V_s is the applied voltage to the system

Equation C.4.1 defines the electrical components of the circuit by Kirchoff's and Faraday's laws. The first term describes the motional electromotive force. The second and third terms deal with the self inductance of the system. The fourth term describes the electrical properties of the system and the final term describes the transformer electromotive forces. *Equation C.4.2* describes the force of the system, both mechanical and magnetic. F_s is the applied force acting on the moving slab. The second two terms describe the force per unit length acting on the the rod by the magnetic field. This field acting on the bar is comprised of the induced as well as the applied magnetic fields.

During this analysis Namias is able to give an answer for the first two questions above. The motional emf can be written as $\mathbf{B}_a lv$, provided the self induced emf is included with a varying self-inductance properly accounted for inside the time derivative [24]. The remaining four questions are partially answered in the maths presented in the paper. The third term of *equation C.4.2* is the term which answers the third question posed above. It is noted that the induced

magnetic field must play a role on the system but not in its entirety. It can be shown that it comes out at half the amount, therefore the term is put over two.

Namias then describes a system including the source of the magnetic field $\mathbf{B}_a$. For this system Namias derived the conservation of power for this system as:

$$\begin{aligned} V_{s_1} i_1 + V_{s_2} i_2 + F_s v = & \\ & \frac{d}{dt}\left(\frac{1}{2}mv^2\right) + Ri_1^2 + R'i_2^2 + \frac{d}{dt}\left(\frac{\mathbf{B}_a^2 ld}{2\mu_0}\right) \\ & + \frac{1}{2}\mu_0 i_1^2 vl + i_1 v\mathbf{B}_a l + \mathbf{B}_a lx\frac{di_1}{dt} \\ & + i_1 lx\frac{d\mathbf{B}_a}{dt} + \mu_0 lxi_1\frac{di_1}{dt} \end{aligned} \tag{C.4.3}$$

where:

- i_1 is the current induced in the rod and rail
- i_2 is the current that produces the field $\mathbf{B}_a$
- R is the resistance of the rod and rail
- R' is the resistance of the system producing the field
- V_{s_2} is the source for producing the field

In *equation C.4.3* the left hand side is equal to the power produced or absorbed by the mechanical and electrical sources. The first term on the right hand side of *equation C.4.3* is the rate of change of kinetic energy of the moving slab. The next two terms are the losses due to heating of the conductors. The last six terms on the right hand side represent the rate at which the stored magnetic energy changes in the system [24]. Namias introduces the principle of flux compression with the same example as in *figure C.5* but with certain limitations on the system.

- The initial current i_0 is set up when the moving slab is at $x = x_0$
- There is no voltage source
- The load resistance is zero

- The resistivity of the wall and moving slab is also zero
- Initial magnetic field inside the system is $\mathbf{B}_0 = \mu_0 i_0$
- There are no externally applied fields

With these initial parameters there will be conservation of flux, by:

$$\mathbf{B}A = \mathbf{B}_0 A_0 \tag{C.4.4}$$

If a velocity is now applied to the rod moving in a negative direction, flux compression will start to occur. As the slab moves there is an increase in magnetic pressure at a rate of $1/x^2$, as a result the moving slab will eventually come to a stand still. The solution for the velocity of the moving slab is given by:

$$v = \pm\sqrt{2\eta\big[(1/x_0) - (1/x)\big] + v_0^2} \tag{C.4.5}$$

η is defined as:

$$\eta = \mu_0 \frac{x_0^2 i_0^2}{2m} l = \frac{x_0^2 \mathbf{B}_0^2}{2\mu_0 m} l \tag{C.4.6}$$

The initial plus and minus sign represent the different times during the compression stage. The minus sign is for the time from zero up to the point of turnaround, the positive sign is from the turn around time till infinity. It is useful to know where the rod will stop and in many cases start to move away from the compressed magnetic flux. At this point it is also possible to define the maximum field that will be obtained as well as the amplification factor of the system. The point at which the moving slab will turn around is:

$$x_T = \frac{x_0}{(1 + v_0^2 x_0/2\eta)} \tag{C.4.7}$$

The magnetic field is a maximum at the turn around time and is defined by:

$$\mathbf{B}_m = \mathbf{B}_0 \frac{x_0}{x_T} = \left(1 + \frac{v_0^2 x_0}{2\eta}\right)\mathbf{B}_0 \tag{C.4.8}$$

where the amplification factor $K = \big(1 + \frac{v_0^2 x_0}{2\eta}\big)$, which can also be described as:

$$K = 1 + \frac{\big(\frac{1}{2} M v_0^2\big)}{\big[V\big(\frac{\mathbf{B}_0^2}{2\mu_0}\big)\big]} \tag{C.4.9}$$

where:

- M is the mass of a length of slab Z
- V is the volume defined by $l x_0 Z$

C.4.1 Rod and rail design analysis

In producing meaningful results from the equations stated above a design analysis of a rod and rail system will now be performed. In this design of a generator only an ideal case will be used as this keeps the working relatively simple but does highlight some of the principle concepts for a flux compressor design. The following design parameters will be used:

- The whole system is constructed of copper
  - density (ρ) – 8.9×10^3 kg/m^3
  - resistivity ($\Omega\cdot$ m) – 1.68×10^{-8}
- Dimension:
  - length – 1 m
  - width – 0.2 m
  - height – 0.2 m
  - thickness – 0.01 m
- Initial position of rod - $x_0 = 1$ m
- The walls and rods resistance is zero

A couple of variations will be presented for a complete understanding of the process using the rod and rail system. If the initial field in the volume is equal to 1 Wb/m^2 and the initial velocity is 1000 m/s towards the fixed wall, then the systems performance is as follows.

- $\eta = 22353.2$
- The turn around position, $x_T = 0.043$ m
- The amplification factor $K = 23.37$
- The maximum field $\mathbf{B}_m = 23.37$ Wb/m^2

Keeping the initial seed field as 1 Wb/m^2 and the generator dimensions as mentioned above, *figure C.6* shows how the turn around position and the maximum field varies with different initial rod velocities. The turn around point shown is the distance the rod is away from the fixed wall. *Figure C.7* shows how the velocity of the rod decreases in an exponential curve as it reaches the turnaround point.

If the initial velocity is kept at 1000 m/s and the initial seed field is varied then the resulting maximum field and turning point are shown in *figure C.8*. What can be seen is the turning point occurs further away from the fixed wall. This is due to the increased pressure on the rod from the magnetic field . The starting pressure increases with the increased seed field but also grows much faster than systems with a low starting seed field. There will be a point where the initial velocity on the rod is insufficient to move the rod because of the initial magnetic pressure; as a result no compression of the volume and flux will occur. The maximum field graph is almost parabolic in nature, which is a result that Knoepfel and Novac had predicted.

Figure C.9 shows the effect velocity has on the peak field obtainable from

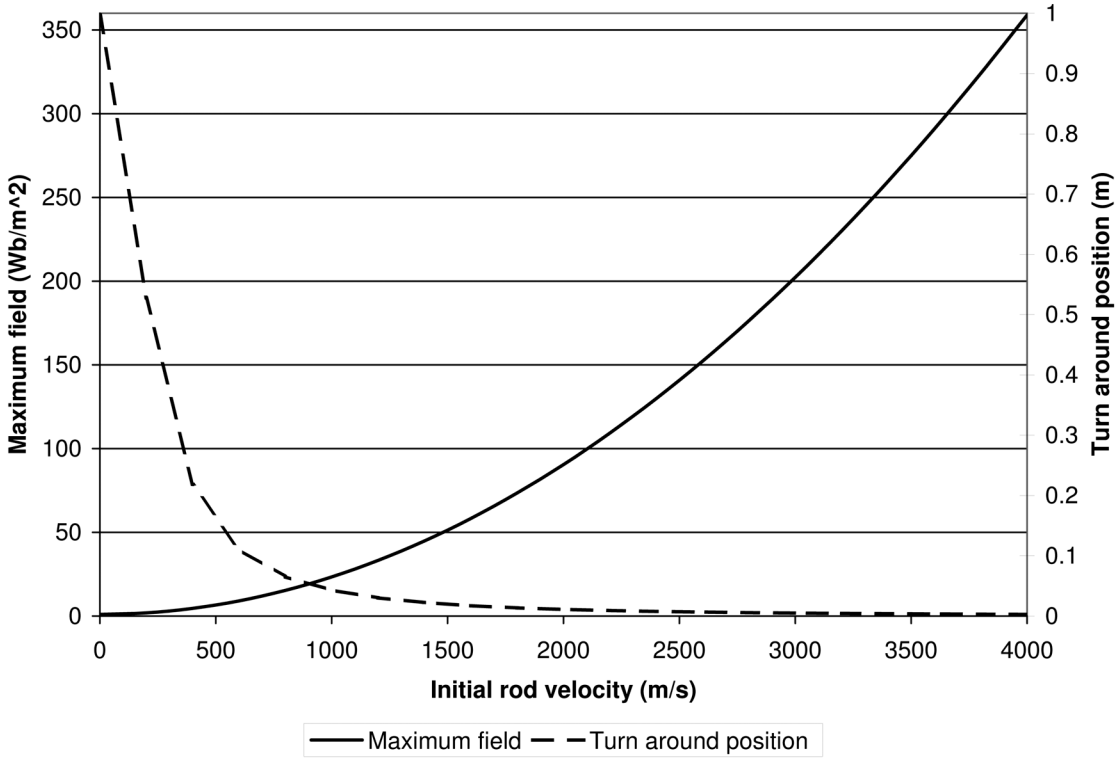


Figure C.6: A graph showing the relationship of the initial velocity of the rod to the maximum field obtainable and the turn around position of the rod.

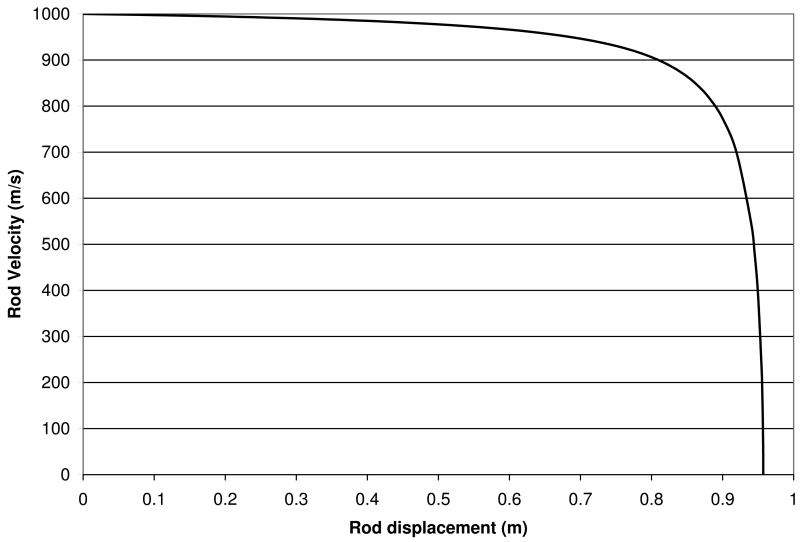


Figure C.7: Graph showing the velocity of the rod as it approaches the turn around point.

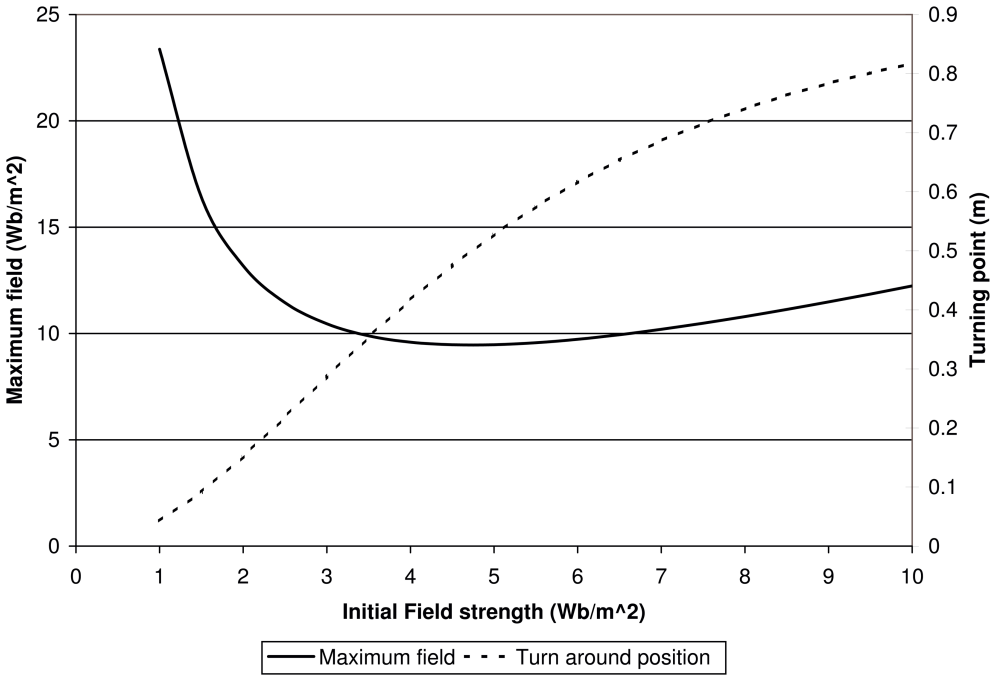


Figure C.8: Graph of the maximum field and the turn around point in relation to the initial field strength.

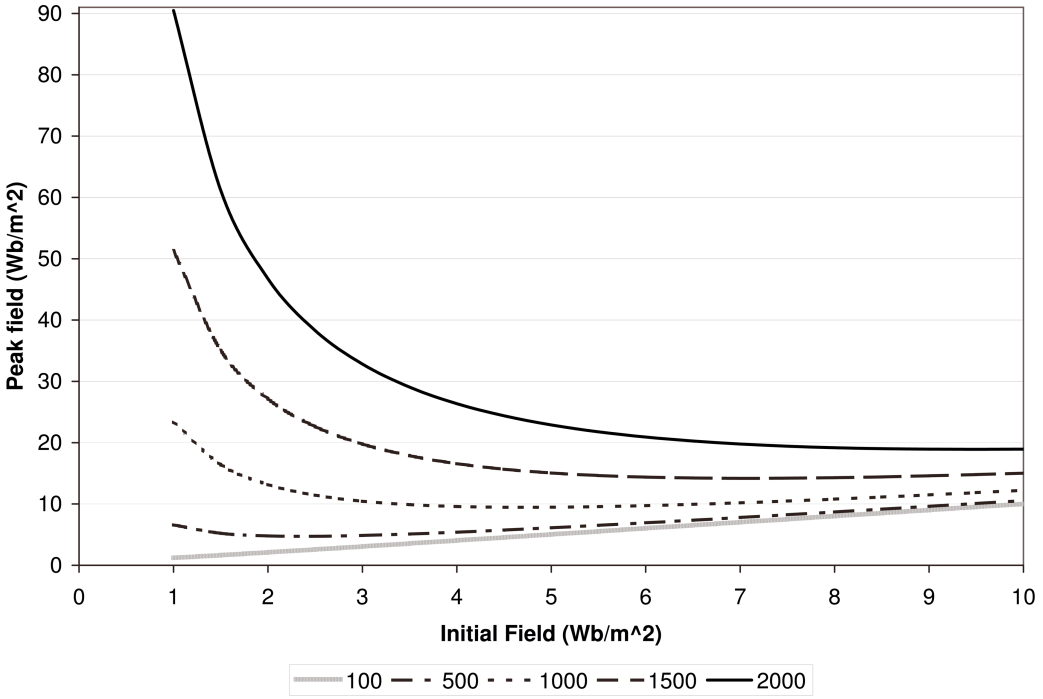


Figure C.9: Graph showing curves relating to different initial rod velocities for a varying initial magnetic field.

various initial fields. Therefore in any generator design there is a balance that needs to be taken into account. If the initial liner velocity is very high, a higher initial seed current could be used. However for a greater gain a smaller seed field would maximise the generator performance.

C.5 Implosion of a cylindrical ideal flux compressing shell

For the generation of high magnetic fields it is often easier to implode a cylindrical liner. It is again possible to express the equations for an ideal case, based on the two diagrams shown in *figure C.10*. There are two stages shown, the first is at $t = 0$ and the second is after $t = 0$ and before the turn around time. There is an initial field set-up in the cylinder which is then compressed. The system is ideal so the flux is conserved and therefore the field amplification is:

$$\frac{\mathbf{H}}{\mathbf{H}_0} = \left(\frac{R_1}{r_1}\right)^2 \tag{C.5.1}$$

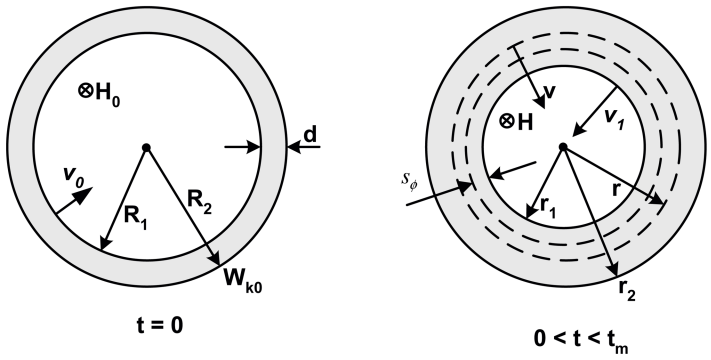


Figure C.10: An ideal shell (a) before and (b) during implosion [4].

The initial magnetic energy is described by:

$$W_{Mo} = \frac{1}{2}\mu_0 \mathbf{H}_0^2 \pi R_1^2 \tag{C.5.2}$$

The kinetic energy of the liner is transformed into magnetic energy and at the turn around point there is only magnetic energy defined by:

$$W_{Ko} + W_{Mo} = \frac{1}{2}\mu_0 \mathbf{H}_t^2 \pi r_t^2 \tag{C.5.3}$$

where the subscript "t" indicates the turn around values. The kinetic energy is described by:

$$W_{Ko} = \pi \rho^2 v_0^2 R_1^2 \ln\left(\frac{R_2}{R_1}\right) \tag{C.5.4}$$

$$\frac{\mathbf{H}_t}{\mathbf{H}_0} = \left(\frac{R_1}{r_t}\right)^2 = \frac{W_K o}{W_M o} + 1 \tag{C.5.5}$$

There is an initial potential energy of the the initial magnetic field which applies a pressure on the walls of the cylinder. This pressure is defined as:

$$p_1 = \frac{1}{2}\mu_0 \mathbf{H}^2 = \frac{1}{2}\mu_0 \mathbf{H}_0^2 \left(\frac{R_1}{r_1}\right)^4 \tag{C.5.6}$$

The potential magnetic energy is equal to:

$$W_m - W_{Mo} = \pi R_1^2 \frac{1}{2}\mu_0 \mathbf{H}_0^2 \left(\frac{R_1^2}{r_1^2} - 1\right) \tag{C.5.7}$$

C.6 Types of flux compressors

There are a couple of different names that are associated with flux compression generators. In most cases the device is called a flux compression generator

(FCG) or an MFCG where the "M" stands for magnetic. It can also be referred to as a magnetocumulative generator (MCG). Most modern systems are helical in design and therefore are called HFCGs. MCGs are generally divided into two classes [23]:

- High-energy density or field generators, which generate very high magnetic fields through the compression of a cylindrical liner
- Current or energy generators, which have inductive loads which are separated from the compressed volume.

The two most common designs of MCGs used are those first proposed by Sakharov, in the form of the MK-1 and MK-2 generators. There are however many generators with slight modifications on these designs. They are listed below [23] and will not be considered further in this work.

- Coaxial – CMCG
- Spiral (Helical) – SMCG (HMCG)
- Plate – PMCG
- Loop – LMCG
- Disk – DMCG
- Shock wave or semiconductor – SWMCG

C.6.1 Sakharov's MK-1 generator

Designed for the production of high magnetic fields The MK-1 generator is an explosive driven imploding liner design. *Figure C.11* shows the basic set-up of the MK-1 generator. Its design consists of a primary source, which is usually a capacitor bank. This feeds into a solenoid for generating the initial seed field. The field is formed inside a hollow conducting cylinder. It was found to be convenient to cut a slit in the cylinder to allow for a faster penetration of the field into the volume of the cylinder. Finally the HE is used to compress the cylinder. As the cylinder compresses the gap is closed and the trapped flux is

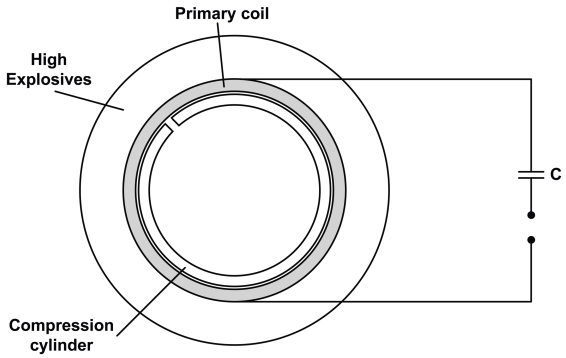


Figure C.11: Diagram of the MK-1 generator.

compressed. Initial experiments performed on the MK-1 yielded a final field of 100 T from a seed field of 3 T [1].

C.6.2 Sakharov's MK-2 generator

The second design of Sakharov is the MK-2 which is also an explosive driven system. However in this case the liner is packed with the explosives and causes an outward acceleration of the liner. The liner expands outwards and makes contact with the helical coil. As this explosion moves down the length of the tube more and more coils are shorted out finally leaving a single turn volume. The flux is compressed in this volume producing a large impulse current that can be used on a load. *Figure C.12* shows the schematic of an MK-2 generator. Early experiments done with this design generated currents up to 100×10^6 Amperes [1].

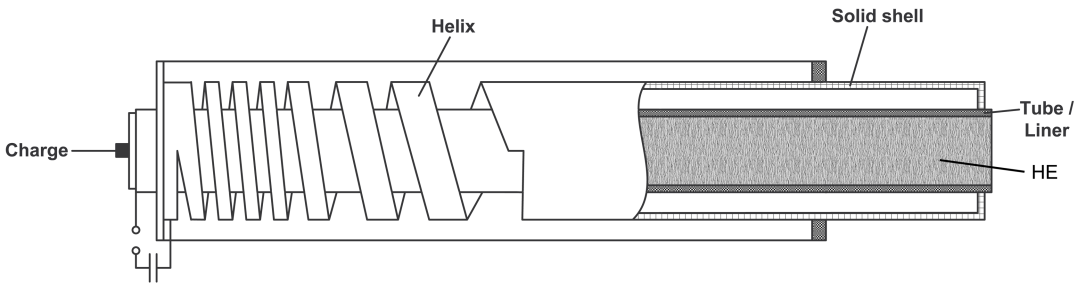


Figure C.12: Diagram of the MK-2 generator [1].

C.6.3 Explosive flux compression

If the induction law is applied to a conducting cylinder through which current flows, from Faraday's law the equation is:

$$\oint \mathbf{E}.ds = -\frac{d}{dt}\int \mathbf{B}.dA \tag{C.6.1}$$

From this equation looking at the first approximations and replacing the left hand side of *equation C.6.1* with $2\pi r\rho\mathbf{B}/\mu_0\delta$ the equation for the field can be represented by [2]:

$$\mathbf{B} = \mathbf{B}_0 \exp\left(\frac{-t}{\tau_0}\right) \qquad \text{where} \quad \tau_0 = \frac{\mu_0\delta r}{2\rho} \tag{C.6.2}$$

Equation C.6.2 actually represents an exponentially decaying magnetic field. It is in fact the time dependence of the equation that is important. This therefore points to the fact that if the liner is deformed very quickly in relation to the time needed for the flux to dissipate through the liner, then flux compression is possible. The following equation from Erber and Latal's work [2], indicates that flux compression is possible even without superconductors.

$$\mathbf{B}_f \simeq (\mathbf{B}_i)_{av}\left(\frac{A_i}{A_f}\right)^{1-(\tau/\tau_0)} \qquad \text{where} \quad \tau < \tau_0 \tag{C.6.3}$$

From this it is possible to show that flux compression is possible as long as the velocities required for flux compression are in the order of:

$$v \simeq \frac{\left|A_i^{\frac{1}{2}} - A_f^{\frac{1}{2}}\right|}{\tau_0} \tag{C.6.4}$$

Erber and Latal show that the minimum liner velocity required for flux compression to occur is $v \gtrsim 0.3$ km s^{-1}= 0.3 mm μs^{-1} [2]. The relationship is one of the fundamental reasons most systems use high explosives as the initial energy source.

C.6.4 Electromagnetic implosive devices

An alternative to Sakharov's initial design is the introduction of using electricity to compress the conductor. These generators are specifically designed for the production of very high magnetic fields. There are two classes of this type of generator; they are ϕ–implosion and z–implosion as seen in *figures*

C.13 & C.14 respectively. The steps that occur during the operation of an electromagnetic generator are [2]:

1. Capacitor bank discharge into single turn coil
2. Two equal but opposite currents are realised in the liner and coil
3. Due to the mechanical asymmetry the liner is imploded concentrically

Liner velocities as large as 1 mm μs^{-1} are possible. Erber *et al* noted that through experimentation the peak values of the compressed field are of the order of:

$$\mathbf{B}(MG) \simeq 0.25E^{\frac{1}{2}}(kJ) \tag{C.6.5}$$

where E is the energy of the capacitor bank. Though this gives a relative value of the expected field experiments performed by Alikhanov, Cnare is not in complete agreement [25]. The equation of motion which describes the

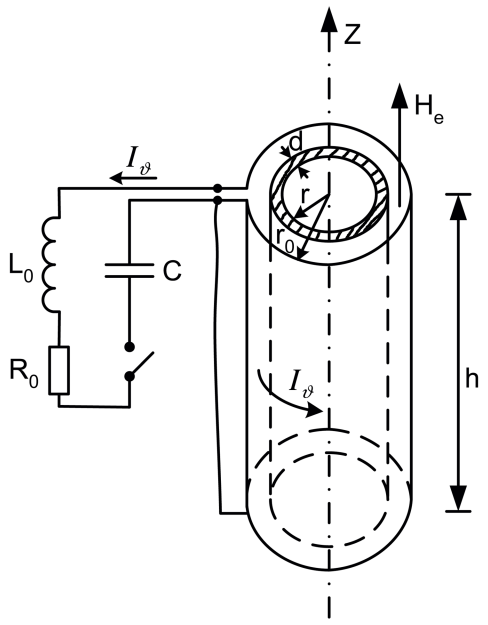


Figure C.13: θ – implosion generator set-up [4].

implosion of the liner in both cases is [4]:

$$-m\frac{d^2r}{dt^2} = \frac{1}{2}\mu\mathbf{H}^2 2\pi r, \tag{C.6.6}$$

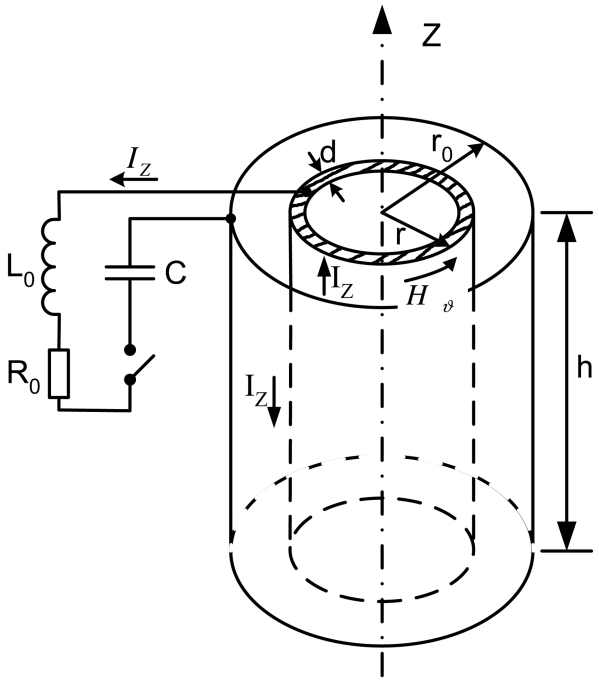


Figure C.14: z – implosion generator set-up [4].

where $m = 2\pi r_o d_0 \rho$ is the mass per unit length of the incompressible liner. For each of the different set-ups the respective fields produced within the generator are defined by:

$$\mathbf{H} = \mathbf{H}_0 = \frac{I}{h} \qquad \text{for} \quad \theta - \text{implosion} \tag{C.6.7}$$

and

$$\mathbf{H} = \frac{1}{2\pi}\frac{I}{r} \qquad \text{for} \quad Z - \text{implosion} \tag{C.6.8}$$

Using the above three equations it can be shown for a particular equation that if the current in the circuit remains constant, $(I = I_c)$. The velocity of the liner for a z-implosion liner is defined by [3]:

$$v_f \approx \sqrt{\frac{\mu}{16\pi}} I_c \left(\frac{1}{m} \ln \frac{r_0}{2d_0} \right)^{1/2} \tag{C.6.9}$$

For a θ-implosion generator the final velocity is defined as:

$$v_f = r_0 A \tag{C.6.10}$$

where

$$A = \sqrt{\frac{\pi\mu}{m}} \frac{I_c}{h} \tag{C.6.11}$$

It can be seen from this therefore that the θ-implosion final velocity is far smaller then that for a z-implosion set-up. This can be seen in *table C.1*, which are results recorded from work performed by Knoepfel [4].

Source and results	Dimensions	θ-implosion	z-implosion
Energy Source			
bank energy W_{CB}	kj	136	570
bank voltage U_0	kV	20	4.8
maximum bank current I_m	MA	0.64	4.9
characteristic discharge time (T_0)	μs	25	40
Initial conditions			
shell material		Al	Cu
shell radius R_1	cm	3.95	3
shell thickness d_0	cm	0.08	0.2
shell length l_0	cm	2	15
initial field $\mu\mathbf{H}_0$	T	2.5	3.5
Results			
maximum implosion velocity (around r_m)	cm/μs	0.17	0.13
corresponding radius r_m	cm	0.3	0.33
total implosion time t_f	μs	33	63
maximum measured field $\mu\mathbf{H}_m$	T	110	280

Table C.1: Results from electromagnetic implosion generators.

C.7 Flux compression - according to Levi

The process of flux compression can be divided up into many different parts, in some cases being very small but definite actions. These many parts can be compiled into three main steps:

1. The build up of initial flux interlinkage, $L_0 i_0$ or field excitation
2. The flux compression and accompanying current rise
3. The current decay

C.7.1 Initial field generation

There are various ways of setting up the initial field required for compression. One of the most obvious ways is that of permanent magnets. There are however certain limitations to this, the most obvious is that of limited field strength. Though these may work for low powered generators their real world

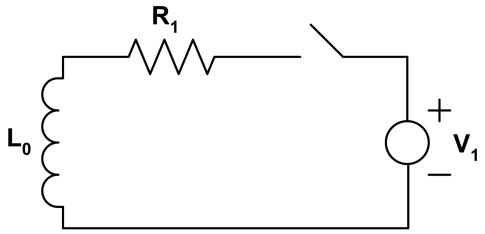


Figure C.15: Seed field circuit.

applications are very few. The use of an R-L circuit to develop an initial field is far more useful and has greater range of field strengths. The defining equation for the circuit in *figure C.15* is:

$$L_0 \frac{di}{dt} + R_1 i = V_1 \tag{C.7.1}$$

and solving for the current in the circuit gives:

$$i(t) = \frac{V_1}{R_1}\left(1 - e^{-\frac{R_1}{L_0}t}\right) \tag{C.7.2}$$

In order to obtain good efficiency of the initial field generation the current build up time should be less then the circuit time constant L_0/R_1 [26].

C.7.2 Flux compression

Figure C.16 shows the circuit including a crowbar switch. In this case the current is defined by:

$$i = i_0\left(\frac{L_0 - at}{L_0}\right)^{\frac{R_2 - a}{a}} \tag{C.7.3}$$

where $a = \frac{L_0 - L_1}{T}$. Levi continues to discuss the process of the electrical en-

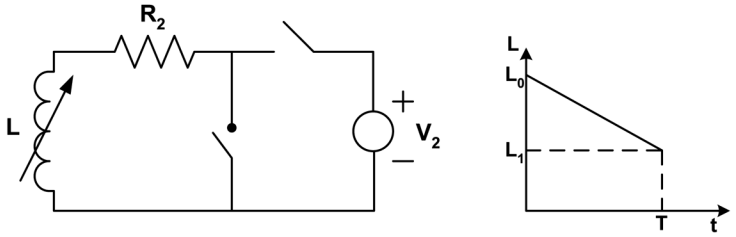


Figure C.16: Circuit including a crowbar switch and a graph showing the time varying inductance over time.

ergy to the mechanical energy and with a crowbarred source the final energy relationship is of the form:

$$\frac{\left(W_{el}\right)_{tot}}{W_{m0}} = 1 + \frac{1}{2\frac{R_2}{a} - 1}\left[1 - \left(\frac{L_1}{L_0}\right)^{\frac{2R_2}{a}-1}\right] = EG \qquad \text{(C.7.4)}$$

This is referred to as the electrical energy gain (EG). During this flux compression stage most of the mechanical work done is actually converted to magnetic energy to be converted into electrical energy during the current-decay phase [26]. Levi notes that the energy dissipation within the conductors is much higher then in conventional generators therefore indicating greater losses. The level of gain is also somewhat lower than conventional generators as the ratio of L_0/L_1 is generally no greater than 10.

C.8 High-Voltage MCG systems

Generators have been designed for the generation of high-voltages. In some however there is a necessity for a higher output and therefore the inclusion of some external device may be required. Work has been performed by the Los Alamos National Laboratory (LANL) using transformers between the load and generator [23]. Another method for increasing the voltage is through flux trapping. For the generator to deliver high powers to a load it must have a high change of inductance dL/dt.

C.8.1 Magnetic flux trapping

Multi-stage MCGs use flux trapping to generate high-voltage electrical pulses. Flux trapping occurs when the magnetic energy generated in one circuit is transferred into another circuit and amplified [23]. One of the major advantages of flux trapping systems is the reduced weight through no need for a transformer. Systems of this type have achieved magnetic flux amplification up to 310 times, and energy increases by a factor of 10^6.

Flux trapping systems experience major problems when it comes to the design and application of the device. Using the method of trapping flux, incredibly

high electrical fields are generated. If there is breakdown between the liner and the stator section then the output impulse is all but lost [7]. The insulation required to prevent breakdown must be sufficient between the turnings of the stator section and between the stator and liner. There is however a problem with making the insulation too thick as uncompressed flux will be present in the space between the coils after the flux compression. The efficient operation of such a system also requires that the initial generator inductance is high which becomes a problem when the load has a high impedance.
High precision in manufacturing is very important as it affects the flux losses in the system. If the expanding liner does not form a cone shape and remain coaxial to the stator there is a possibility that the contact point may jump forward and as a result the flux trapped between the two contact points is lost (2π-clocking) [23].
Work has been performed by Sheildlin and Fortovon on MHD generators with regard to their physical construction and the alignment in most cases must be within a measurement of 0.1 mm [23]. However the surface finish of the liner is not as critical to the generators performance [7]. Experiments were performed on the following generator designs:

- Simultaneously axially initiated MCG
- Cylindrical spiral MCG
- Conical spiral MCG

C.9 The use of transformers on electrical loads

MCGs are used to drive various loads such as plasma focus mechanisms, high power lasers and electromagnetic launchers [23]. The characteristics of the load and MCG will affect how the two devices are coupled.

C.9.1 Direct connection to a load

Direct connection means that there are no pulse forming devices inserted between the generator and the load. The diagram in *figure C.17* is the equivalent

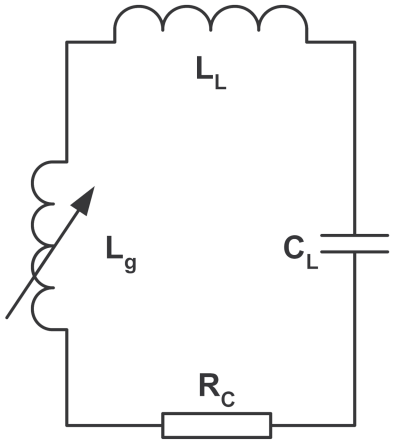


Figure C.17: Equivalent circuit diagram for an MCG [23].

circuit diagram for an MCG connected directly to a load.

The load impedance is $Z = R + jX$, where R is the active (time-dependant) resistance. jX is the imaginary component of the load impedance.
$L = L_g(t) + L_L$, where $L_g(t)$ represents the changing inductance of the MCG and L_L is the load inductance. R_C is the circuit resistance including all magnetic losses as well as the resistance of the load. C_L is the capacitance of the load. The decreasing of the inductance of the MCG greatly affects the characteristics of the series connected LRC circuit. The following defines the circuit operation:

$$L\frac{d^2I}{dt^2} + \left(2\frac{dL}{dt} + R_c\right)\frac{dI}{dt} + \left(\frac{d^2L}{dt^2} + \frac{dR_c}{dt} + \frac{1}{C_L}\right)I = 0 \tag{C.9.1}$$

The voltage on the capacitor is given by:

$$L\frac{d^2U}{dt^2} + \left(\frac{dL}{dt} + R_c\right)\frac{dU}{dt} + \frac{U}{C_L} = 0 \tag{C.9.2}$$

In the book by Altgilbers [23] the above two equations are solved for five different cases with different combinations of the resistance and inductances.

C.9.2 Connection through pulsed transformers

Work performed at LANL using transformers matched to the load impedance, have produced the following results [23]. In the first experiment a vacuum diode was the load and a voltage of 1.2 MV with a pulse rise time of 300 ps

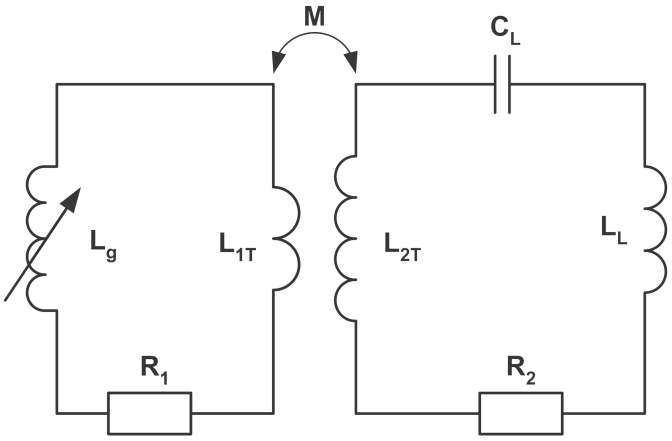


Figure C.18: Equivalent circuit diagram for MCG connected through a pulsed transformer to a complex load [23].

was produced across the vacuum diode. The initial operating voltage of the generator was 35 kV. In the second experiment 1.1 MV was produced across a 25Ω load. This generator had an operating voltage of 40 kV. As in the above case many scenarios are possible. However for this work the primary interest is in a complex load coupled to the MCG through a transformer. A circuit diagram for this set-up is shown in *figure C.18*.

In this circuit the following are the relevant circuit parameters.

- L_1 and L_2 are the inductances on the primary and secondary sides.
- $R_!$ and R_2 are the resistances on the primary and secondary sides.
- L_g and L_{1T} are the generator and transformer primary inductances respectively.
- L_{2T} and L_L are the transformer secondary and load inductances respectively.
- I_1 and I_2 are the respective currents in the primary and secondary circuits.

From this the total inductances per side are defined by $L_1 = L_g + L_{1T}$ and $L_2 = L_{2T} + L_L$and the complete circuit equations can be defined by:

$$L_1 \frac{dI_1}{dt} + \left(\frac{dI_1}{dt} + R_1 \right) I_1 + M \frac{dI_2}{dt} = 0 \qquad \text{(C.9.3)}$$

$$L_2\frac{d^2I_2}{dt^2} + R_2\frac{dI_2}{dt} + \frac{I_2}{C} + M\frac{d^2I_1}{dt^2} = 0 \tag{C.9.4}$$

It is possible [23] to drive a capacitive load if certain conditions are met. The operation of the MCG has to be different to that of driving an inductive or resistive load. One of the main differences is an oscillatory component that is introduced by the capacitance. When the MCG operates in an oscillatory mode, its energy yield increases slowly. In the case of an aperiodic mode, the energy is mainly accumulated in the inductance [23].

C.10 Summary

An ideal generator has relatively simple equations defining the operation of flux compression. What is considered important is the velocity of the liner and the change of inductance. By designing a generator around both of these characteristics it should be possible to produce a generator with a very good performance. Two main methods provide the initial energy for the flux compression, either high explosives or a large capacitor bank. Sakharov's generator designs, the MK-1 and MK-2 were presented and it can be seen that most modern day researchers still rely heavily on these two designs. Flux-trapping or the inclusion of a transformer are methods available to drive larger loads with an impulse form an FCG. From this theory it is possible to design models for the accurate prediction of the results expected from an FCG. Two of these models will be dealt with in the next section.

Appendix D

Ideal theory for any design can provide a relatively useful guide to its performance. However in most cases where a single experiment requires a lot of time and money it is important to be able to have an accurate model to simulate the design before a physical model is built. The theory was dealt with in the previous section and this section presents two models developed at Loughborough University. The first model is a simple model and then second model is based on work performed for the simple model and provides a very comprehensive model for a helical FCG.

D.1 FLEXY I Design, construction and testing

FLEXY I is a helical flux compression generator that was constructed at Loughborough University in the United Kingdom. It was designed by the Authors of the book on Magnetocumulative generators [23]. *Figure D.1* shows a schematic of the main components of the generator as well as the part way through its operation. The explosives are end initiated and the initial electrical source is from a capacitor bank. The following list gives a step by step detail of the FLEXY I operation:

- The source (capacitor bank) sets up the initial field in the generator
- The explosive is detonated
- The armature expands in a conical form which crowbars the source at the time when the maximum current is flowing in the stator
- The armature starts to compress the flux with two processes involved:

  - Kinetic energy from the explosive provides energy to the armature
  - The armature in turn does work against the magnetic field
- The explosive continues down the length of the armature
- Subsequent stator turns are shorted out thus reducing the inductance of the generator
- The load current increases because of the conversion of the armature kinetic energy into magnetic energy

Due to the high initial energy density of the high explosive it is possible even with a fraction of this energy being converted in magnetic energy to get a high output energy.

D.2 FLEXY I Computer models

Two models were produced at Loughborough University and these will be discussed below, these models are:

- A simple design of a 1 MJ generator [23]
- A complete 2-dimensional (2D) model for a helical generator [23]

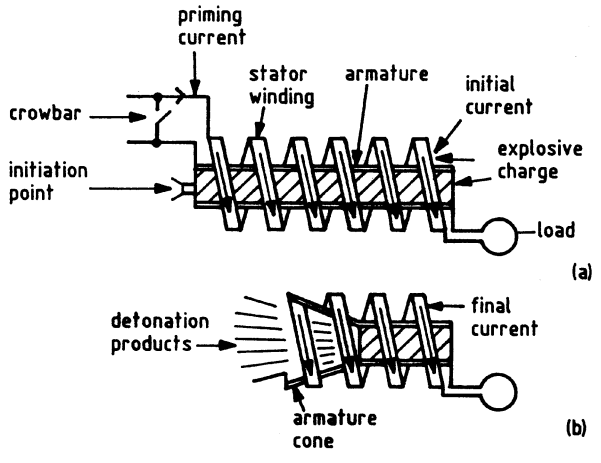


Figure D.1: FLEXY I schematic (a) before detonation and (b) during detonation [23].

A simple general model was initially produced by this group as experimental data was easily produced for verification on medium to large generators. In doing this it made it possible for them to accurately generate a 2D model for the design of mini and micro helical generators.

D.2.1 A simple general model for a helical MCG

This model was designed to give a reasonably accurate prediction of the generator without the long run times required by other models. It is important for the mathematical model to provide adequate accuracy in determining the initial conditions as well as the general performance of the generator. High intensity magnetic and electric fields are generated during flux compression [23], but it is possible to neglect the magnetic effects on the armature and conductor for both small and medium-energy generators. Turn-splitting is used to control the field intensity in these devices. The electric fields cannot be ignored as the potential developed between the stator and armature affects the final results. Inequalities between modelled data and physical results is evident, indicating the influence the electric field has on the system. A maximum voltage is set, this is the upper limit allowed to develop between the stator and the armature (V_{max}). The following equation describes the inductance as it varies from the time that the source is crowbarred [23].

$$L = L_0 \exp\left\{V_{max}\frac{1-\exp(\gamma t)}{L_0 I_0 \gamma} - \gamma t\right\} \tag{D.2.1}$$

Where:

- I is the load current
- Subscript 0 indicates initial conditions
- γ is the ratio of R to L, which is assumed to be constant

Though this equation gives a workable result it does however have its limitations as the L to R values will vary during generator operation and therefore γ varies greatly with time.

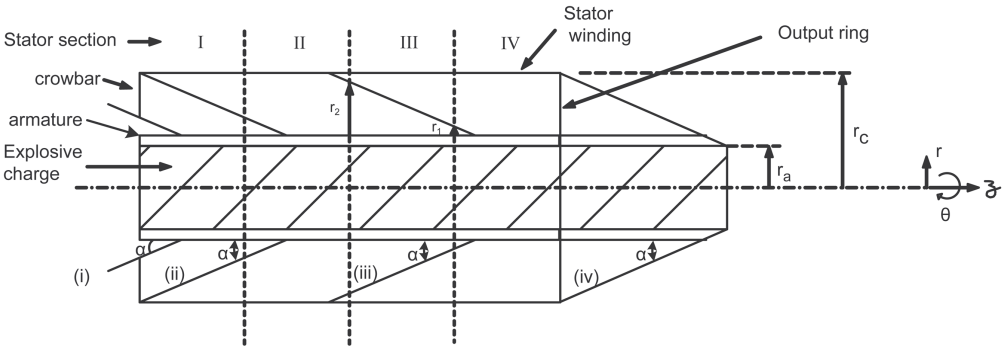


Figure D.2: A four-section generator [23].

A better method to determine the parameters for the generator is by the following equations:

$$L\frac{dI}{dt} + I\frac{dL}{dt} + IR = 0 \tag{D.2.2}$$

$$R = R\left(t, I, \frac{dI}{dt}\right) \tag{D.2.3}$$

$$L = L(t) \tag{D.2.4}$$

The second term in *equation D.2.2* is the energy conservation term and describes the maximum voltage that is induced in the generator [23].

The generator design in *figure D.2* is a representation of the simple generator model being described. The generator is divided up into four equal sections, each with the same number of turns and a constant winding pitch per section. The system can be divided up into two time sections, the first section is the time taken for the armature cone to expand from the crowbar position (i) to position (ii). The second section is the time taken for the contact point to move down the length of the generator to point (iv).

Ohmic Resistance

Ohmic resistance is usually based on the diffusion of the magnetic field into both the magnetic stator coils and the armature. The skin depth δ for the diffusion process can be found by using the following equation [23, 3, 4]:

$$\delta = \left(\frac{I}{\mu_0 \sigma_0 \frac{dI}{dt}}\right)^{\frac{1}{2}} \tag{D.2.5}$$

where:

- μ_0 is the magnetic permeability of free space
- σ_0 is the conductivity of the conductors at room temperature

The equation D.2.5 only holds for an exponential current rise, therefore the solution offers an inaccurate value during the final stages of compression because the current rise is far from exponential. To determine the initial resistance when a capacitor bank generates the initial magnetic field, the skin depth used is given by [23, 3, 4]:

$$\delta = \left(\frac{2\left(L_0 C\right)^{\frac{1}{2}}}{\mu_0 \sigma_0} \right)^{\frac{1}{2}} \tag{D.2.6}$$

where C is the bank capacitance.

The resistance R_c of one section of the helical stator coil can be found by using both a *skin effect factor* f_δ and a *proximity effect factor* f_p [23].

$$R_c = R_{DC} f_\delta f_p \tag{D.2.7}$$

where R_{DC} is the DC coil resistance,

$$f_\delta = \frac{\Phi}{d\delta} \tag{D.2.8}$$

and

$$f_p = \begin{cases} n\left[1 = 2\left(\frac{n\Phi}{\delta}\right)^2\right], \ \Phi \geq 2\delta \\ n\left[1 + \frac{n^5 \Phi^2}{a p^2 \delta^3}\right], \ \Phi < 2\delta \end{cases} \tag{D.2.9}$$

where:

- Φ is the diameter of the wire
- n is the number of parallel paths in a section
- p is the pitch of each section

The current that is seen in the armature forms a reflection of the helix pattern of the stator coils. The armature resistance can be calculated using *equation D.2.9*, but in this case $f_P = 1$. During the first period of the flux compression process there is a rapid increase in the generator's resistance. From *figure D.2* the length of the armature cone can be calculated from section (iii) with the two radii r_1 and r_2. Equations defining a helix on the surface of the armature can be described as follows: cylindrical coordinates (r, θ, z) being introduced,

$$z = \frac{p\theta}{2\pi} \tag{D.2.10}$$

$$r = r_2 - \frac{p\theta \tan\alpha}{2\pi} \tag{D.2.11}$$

The elemental length can be descibed as:

$$dl = \left[(rd\theta)^2 + (dz)^2 + (dz)^2\right]^{\frac{1}{2}} \tag{D.2.12}$$

which can be written as

$$dl = \left[\frac{p\tan\alpha}{2\pi}\right]\left\{\left[\frac{2\pi r_2}{p\tan\alpha} - \theta\right]^2 + \left(1 + \cot^2\alpha\right)\right\}^{\frac{1}{2}} d\theta \tag{D.2.13}$$

The total length l_h of the helix is given by:

$$l_h = \int_{\theta_0}^{\theta_1} \frac{dl}{d\theta} d\theta \tag{D.2.14}$$

where:

- $\theta_0 = 0$
- $\theta_1 = 2\pi(r_2 - r_1)/p\tan\alpha$

Integrating *equation D.2.14* the length is found to be:

$$\begin{aligned} l_h = \frac{1}{2}\Bigg\{ & r_2\left[1 + \cot^2\alpha + \left(\frac{2\pi r_2 \cot\alpha}{p}\right)^2\right]^{\frac{1}{2}} \\ & - r_1\left[1 + \cot^2\alpha + \left(\frac{2\pi r_1 \cot\alpha}{p}\right)^2\right]^{\frac{1}{2}} \\ & + \left[\frac{p\tan\alpha}{2\pi}\left(1 + \cot^2\alpha\right)\ln\frac{R_2}{R_1}\right\} \end{aligned} \tag{D.2.15}$$

where

$$R_1 = r_1 + \sqrt{r_1^2 + \left(1 + \cot^2\alpha\right)\left[\frac{p\tan\alpha}{2\pi}\right]^2} \tag{D.2.16}$$

$$R_2 = r_2 + \sqrt{r_2^2 + \left(1 + \cot^2\alpha\right)\left[\frac{p\tan\alpha}{2\pi}\right]^2} \tag{D.2.17}$$

Inductance

There are many methods of calculating the inductance of a system as has been shown earlier. The method used by Altgilbers *et al.* [23] is based on previous work done by C. M. Fowler *et al.* The main criteria for this method is that the ratio of the diameter of the stator to its length is less than 1.5. The advantage of this system is that it produces an error of less then 5%. The inductance L_s of the stator in relation to its length (l) is:

$$L_s = \frac{k_1 l^2\left(r_c^2 - r_a^2\right)}{p^2\left[l + k_2\left(r_c - r_a\right)\right]} \tag{D.2.18}$$

where

- r_c and r_a are the radii of the coil and armature respectively
- $k_1 = 0.003948$ and $k_2 = 0.45$ are constants

The mutual inductance of the system is far less than the self inductance and can be calculated for adjacent coils x and y from the following equation [23]:

$$M_{xy} = \frac{k_2 L_x p_x\left(r_c - r_a\right)}{p_y\left[2l + k_2\left(r_c - r_a\right)\right]} \tag{D.2.19}$$

In sections where the armature is either expanding or the armature is actually in contact with the stator the following expression should be subtracted from the value of the inductance for that section.

$$\Delta L_s = \frac{k_1\left[r_a\left(r_1^2 - r_2^2\right) + \frac{1}{3}\left(r_1^3 - r_2^3\right)\right]}{p^2\tan\alpha\left\{l + k_2\left[r_c - \frac{1}{2}\left(r_1 + r_2\right)\right]\right\}} \tag{D.2.20}$$

where

- r_1 and r_2 are the radii of the armature cone at each end of the section

- α is the angle of the cone

Some general comments on this model for the inductance calculations:

- lengths are all in millimetres
- Inductance is calculated in microhenrys
- the length of a section is only that area where the stator and armature are not in contact
- The flux density is assumed to be uniform throughout the volume
- Improved accuracy was obtained by replacing $\left(l^2 + 4r_c^2\right)^{\frac{1}{2}}$ by $\left(l + 0.9r_c\right)$
- The self-inductance is much greater then the mutual inductance as the armature moves therefore there is little necessity in calculating this mutual inductance change; the error introduced is minimal

It should be noted that the length of each section is in accordance to that area that the stator and armature are not in contact.

Non-ohmic losses

These include the effects of the non-linear diffusion of the magnetic field, 2π-clocking, geometric defects in the armature and voltage breakdown [23].

Non-linear diffusion of the magnetic field
There are two methods for calculating the inductances and resistances in a helical generator [23].

1. As each turn is removed from the circuit the diffusion of the field into the conductors is seen as a permanent energy loss
2. To neglect the diffusion losses when calculating the inductances, but to include them in the resistance calculations

From the second point the current density is low so the diffusion losses are linear, therefore there is no energy loss at the contact point. At the contact point however there is heating of the wires due to the non-linear diffusion of the magnetic field and therefore losses occur. A modified skin depth is introduced (δ^*) which is calculated from:

$$\delta^* = \delta\sqrt{\frac{1}{T_0}\left(T_0 + \frac{B^2}{\mu_0 \rho c_V}\right)} \tag{D.2.21}$$

where

- T_0 is the initial temperature of the coil
- B is the magnetic flux density arising from the coil current
- ρ is the density of the coil conductors
- c_V is the specific heat of the coil conductors

To derive an expression for the equivalent resistance from this case the following analysis is performed. The inductance related to the change in volume is:

$$\frac{1}{2}I^2\Delta L = \frac{B^2}{2\mu_0}\Delta V \tag{D.2.22}$$

For non-linear diffusion:

$$\Delta V = 2\Delta l(S^* - S) \tag{D.2.23}$$

where

- ΔV is a volume removed form the internal generator volume
- ΔL is the reduction in inductance
- Δl is the cable length removed
- Δt is the time taken
- S^2 and S are circular cross-sectional areas inside the cable defined by skin depths δ^* and δ
- The 2 is included because of the diffusion at the armature as well the coils

The approximate velocity of the contact point is:

$$v_{cp} = \frac{2\pi r_c v_{det}}{p} \tag{D.2.24}$$

From this the equivalent non-Ohmic resistance is:

$$R_n d = \frac{\Delta L}{\Delta t} = 2B^2 c_{cp} \frac{S^* - S}{\mu_0 I^2} \tag{D.2.25}$$

Where the magnetic flux density is calculated from :

$$B = \frac{\mu_0 I}{\pi n \Phi} \tag{D.2.26}$$

The non-Ohmic diffusion for n contact points of the armature with the n cables gives the equivalent resistance of:

$$R_{nd} = \frac{2\mu_0 v_{det}\left[\delta^*(\Phi - \delta^*) - \delta(\Phi - \delta)\right]}{\pi \Phi^2 n \cos\beta} \tag{D.2.27}$$

where

- $\cos\beta \approx p/2\pi r_c$
- β is the angle made by the coil with the plane normal to the coil
- v_{det} is the detonation velocity

If the linear current density flowing along the coil axis is maintained below 0.2 MA/cm it can be shown by calculations and experiments that there is little loss due to magnetic diffusion [23].

$2\pi-$*Clocking*

In the case where the armature and stator are not coaxial, losses occur due to 2π-clocking. The process is a misalignment of the armature and stator as they make contact and as a result the armature can skip turns. This often occurs in the earlier sections of helical generators as the turns are very close together. This is one of the primary loss mechanisms and in some cases is the only loss that needs to be considered [23].

Geometric defects

The machining of the armature can introduce undulations into the metal. At the time when the armature is exploded outwards these undulations will

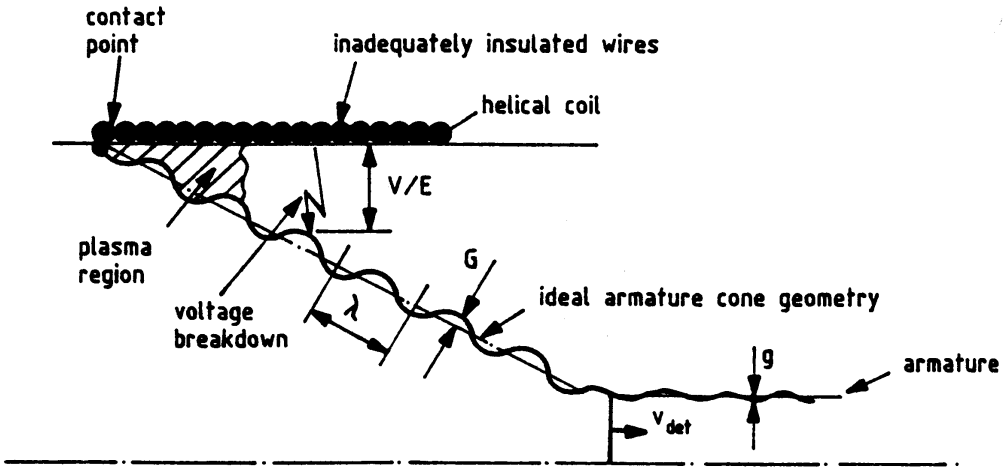


Figure D.3: The effects of geometric defects and the occurrence of voltage breakdown [23].

be exaggerated, creating a sinusoidal leading edge of the liner as shown in *figure D.3*. This increases the losses because of the multiple contact points. The same affect can occur in systems where the liner is made of inhomogeneous material or the armature to stator ratio is very large [23].

Voltage breakdown

Voltage breakdown is seen as the most important of the non-Ohmic losses. Plasma can be formed ahead of the contact point because the electric field intensity is sufficiently high. Breakdown usually occurs ahead of the contact point and the plasma. This occurrence is particularly high in the case of deformities in the armature construction as mentioned above. For a detonation velocity of v_{det}, the equivalent non-Ohmic resistance is [23]:

$$R_{vb} = \frac{2\pi\mu_0 v_{det} A \cos\alpha(2r_c - A)}{r^2} \tag{D.2.28}$$

- A is the effective amplitude of the armature expansion defects in the presence of a voltage breakdown

The magnetic energy is lost to the system between the point of breakdown and the plasma and as a result a new effective amplitude is given by $A = G = V/E$.

From this the total non-Ohmic resistance for a generator is defined as:

$$R_{no} = R_{nd} + R_{2\pi} + R_{vb} \tag{D.2.29}$$

This expression is effective only after the armature has made contact with the coil, for only then does it have any significant effect on the calculated current [23].

D.2.2 Simple 2D model for a Helical MCG

The code developed by Altgilbers *et al.* [23] is easily adapted to model high-energy and high-current generators having a variable geometry for both the helical coil and the armature. The design of a 2D model far enhances the capabilities of the designer to produce a more accurate result and therefore the optimization of any generator is possible. The 2D model allows for the accurate modelling of the effects of the coil armature contact region where the initial flux compression occurs.

The equations

The system is divided into the z and θ currents which produced the flux densities B_z and B_θ. The system can be seen in *figure D.4*. The z circuit consists of the helical coil, armature and load. The helical coil is divided in a certain number of rings. The θ circuit consists of coaxial structure made up of the rings and armature and these generate the b_θ field. From *figure D.4* in the θ-current circuits it is useful to base the number of rings on the number of stator windings, however it is not essential. For this analysis it is assumed that this is the case and it is therefore possible to divide the armature circuit into N+1 equivalent circuits. The following N equations for the load circuit (z) can be described as:

$$L_z\frac{dI_z}{dt}+\sum_{i=1}^{N}\left(M_{zi}\frac{dI_i^\theta}{dt}+\frac{dM_{zi}}{dt}I_i^\theta\right)+\left(R_z+\frac{dL_z}{dt}\right)I_z=0 \qquad \text{(D.2.30)}$$

The equivalent circuit diagram for this equation is shown in *figure D.5*. From this the equation for the θ-circuit is:

$$L_i^\theta\frac{dI_i^\theta}{dt}+M_{zi}\frac{dI_z}{dt}+\frac{dM_{zi}}{dt}I_z$$
$$+\sum_{\substack{j=1\\ j\neq i}}^{N}\left(M_{ij}^\theta\frac{dI_j^\theta}{dt}+\frac{dM_{ij}^\theta}{dt}I\right)+\left(\frac{dL_i^\theta}{dt}+R_i^\theta\right)I_i^\theta=0 \qquad \text{(D.2.31)}$$

By dividing the generator components into small rings. Each component will then go through different processes of which there are defining equations. In breaking the generator design down into these small components it makes the solving of the equations more manageable. This process is shown in *figure D.5* where for each ring the self and mutual inductances can be found. The resistances can also then be calculated for each component in each section. In the conical section dividing the armature and coils into smaller parts any changes are far more easily dealt with. Solving for the resistance and inductance of the system is lumped into conical and cylindrical sections and the generator can be solved for.

Calculating the Inductance
The total inductance of the z - circuit is

$$L_z = L_z^z + L_z^\theta + L_{load} \tag{D.2.32}$$

where

- L_z^z relates to B_z^Z

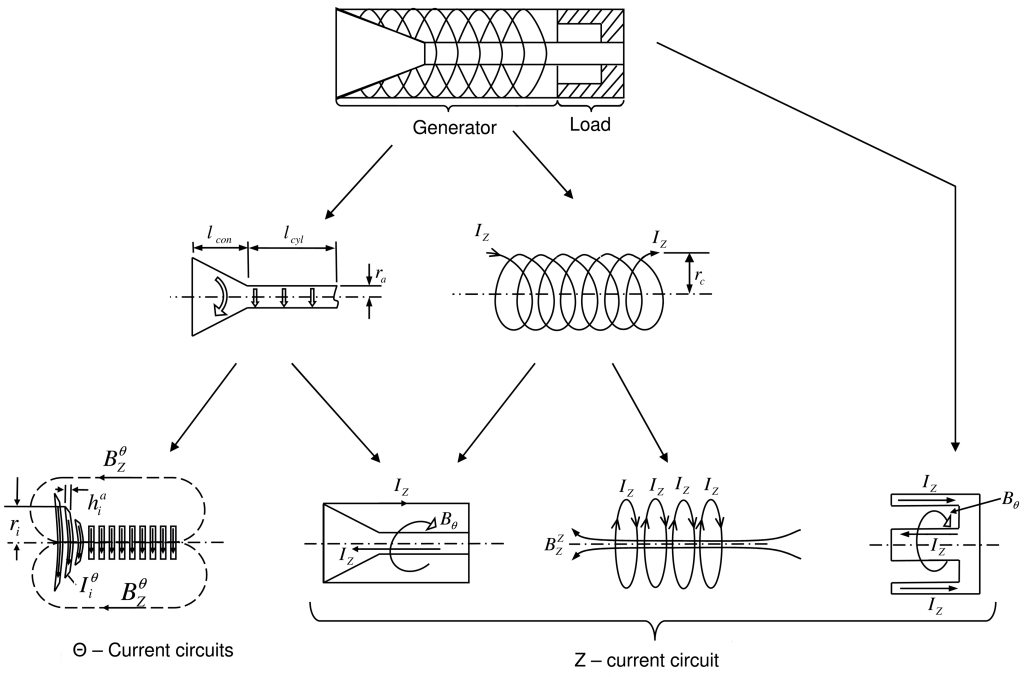


Figure D.4: Decomposition of a helical generator into z and θ circuits [23].

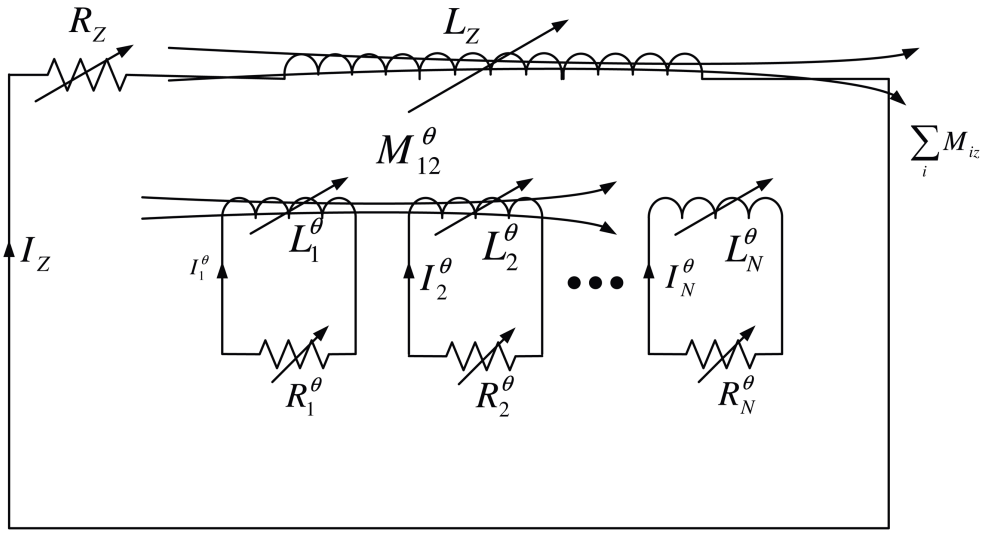


Figure D.5: Equivalent circuit diagram with the armature separated into θ rings.

- L_z^{θ} relates to B_z^{θ}
- $L_z^{\theta} = L_{cyl} + L_{con}$

from the θ circuit the expression for the L_{cyl} and L_{con} are described by

$$L_{cyl} = \frac{\mu_0 l_{cyl}}{2\pi} \ln \frac{r_c}{r_a} \tag{D.2.33}$$

and

$$L_{con} = \frac{\mu_0}{2\pi} K \tag{D.2.34}$$

The subscripts for the inductances relate to the cylindrical and conical parts of the coaxial structure. K is defined by

$$K = l_{con} + \frac{1}{\tan\alpha}\left[r_a \ln \frac{r_a}{r_c} - (r_a + l_{con}\tan\alpha) \ln\left(\frac{r_z + l_{con}\tan\alpha}{r_a} \right) \right] \tag{D.2.35}$$

The B_z^z field is produced from the inductance L_z^Z which is given by

$$L_z^z = \sum_{i=1}^{N} \left(L_i^z + \sum_{\substack{j=1 \\ j\neq i}}^{N} M_{ij}^z \right) \tag{D.2.36}$$

where the inductance of a very thin ring is

$$L_i(r_i, h_i) = \mu_0 r_i \left(\ln \frac{8r_i}{h_i} - 0.5 \right) \tag{D.2.37}$$

- r_i is the radius of the ring
- h_i is the width of the ring in the z-direction

The mutual inductance between two coaxial rings having radii of r_i and r_j is

$$M_{ij}(r_i, r_j, d_{ij}) = \mu_0 \Bigg[- \left\{ \left(r_i + r_j\right)^2 + d_{ij}^2 \right\}^{\frac{1}{2}} E\left(x_{ij}\right) + \frac{\left(r_i^2 + r_j^2 + d_{ij}^2\right) K\left(x_{ij}\right)}{\left\{ \left(r_i + r_j\right)^2 + d_{ij}^2 \right\}^{\frac{1}{2}}} \Bigg] \tag{D.2.38}$$

- d_{ij} is the distance between rings
- E and K are complete integrals of the first and second kind respectively

The modulus for the complete elliptic integrals is:

$$x_{ij} = \frac{4 r_i r_j}{\left(r_i + r_j\right)^2 + d_{ij}^2} \tag{D.2.39}$$

The mutual inductance for the θ-circuit are described by equations similar to *equations D.2.37 - D.2.39.*

Calculating the resistance
The total resistance for the generator circuit is

$$R_z = R_z^\theta + R_z^z + R_z^P + R_{load} \tag{D.2.40}$$

where

$$R_z^\theta = R_{cyl} + R_{con}, \tag{D.2.41}$$

$$R_{cyl} = \frac{l_a}{\pi \delta_a} \cdot \frac{l_{cyl}}{2 r_a - \delta_a} \tag{D.2.42}$$

$$R_{con} = \frac{\rho_a}{2 \pi \delta_a \tan \alpha} \ln \left[\frac{2 l_{con} \tan \alpha}{2 r_a - \delta_a} + 1 \right] \tag{D.2.43}$$

and

$$R_z^z = \sum_{i=1}^{N} R_i^z \left(r_i^c, h_i^c\right) \tag{D.2.44}$$

For the above equations:

- ρ is the electrical conductivity
- δ is the skin depth

- Superscript z and θ represent the helical coil and armature respectively
- R_z^P is a term for the axial length of the helical coils proximity to each other

The resistance in the i^{th} ring is therefore represented by:

$$R_i\big(r_i, h_i\big) = \frac{2\pi\rho r_i}{\delta h_i} \tag{D.2.45}$$

Armature ring dynamics
In order to calculate the time of expansion for each ring the following equation is used.

$$\Delta t_n = \sum_{i=1}^{n-1} \frac{h_i^a}{D} \tag{D.2.46}$$

- D is the detonation velocity

The radial velocity of expansion is obtained from $v_r = D\tan\alpha$ which is constant, however not entirely accurate. There is an impulse expansion initially, which must be determined from either x-rays or photographs. The ring acceleration is given by:

$$a_b(t) = \theta(t - \Delta t_n)\left[V_0\dot{\theta}(t - \Delta t_n) + \frac{V_1}{T}e^{-\frac{t}{T}}\right] \tag{D.2.47}$$

where

- a_n is the acceleration of the n^{th} ring
- $\dot{\theta}$ is the time derivative of the step function θ
- V_0, V_1 and T are parameters that must be fitted to experimental data

For the case of very high-current generators it may be necessary to include the effects of the magnetic pressure that is exerted on the ring. From this a term should be added to *equation D.2.47* which includes the magnetic pressure and the mass of the i^{th} ring.

D.3 Helical generator design

In the previous sections the explanation of Altgilbers *et al* [23, 27, 28] models were presented, with the basic equations for the inductance and resistance presented. The design parameters that were used are stated below.

D.3.1 HFCG Parameters

The information is that used in the creation of their 1 MJ generator:

- Capacitor bank – 250 μ F
- Voltage V_{cb} of 20–30 kV
- L_{load} of 40 nH
- I_{max} of about 7 MA
- Minimum limit on the outer diameter of the armature – 106 mm
  - This is in order to keep the linear current density to approximately 0.2 MA/cm
- rather use copper than aluminium
- Detonation velocity of 8.2 km/s
- Optimal armature wall thickness – 9 mm
- Cone angle – 12°
- Stator inner diameter – 212 mm
  - The coil inner diameter should usually be twice the size of the outer armature diameter
  - For copper a higher ratio can be used
- Crowbar diameter – 146 mm

Taken from Altgilbers *et al.* [23].

It is possible to reduce the generator resistance by excluding the armature from the current return path. The detonation of the armature must also extend past the end of the stator section to prevent inertial movement of the stator.

D.3.2 Design rules

Novac and Smith [23] proposed the following rules to aid in the design of an FCG.

(i) *Constant voltage or constant electric field rule*
This rule specifies the maximum voltage that the generator must not exceed, otherwise premature breakdown is possible. It is generally advisable to work below 125 kV. The introduction of SF_6 into the system can be used to reduce the chance of breakdown. For the 1 MJ designed a maximum voltage of 100 kV was selected.

(ii) *Constant linear current density or constant magnetic intensity rule*
The current density should be kept below 0.2 MA/cm to avoid non-linear diffusion losses.

(iii) *The containment rule*
The movement of cables within the coil should be limited to prevent 2π-clocking.

D.4 Network mesh model for a FCG

Work performed in Italy looked at the creation of a network mesh model for the analysis of the behaviour of a magnetic flux compression generator. The experimental set-up of the modelled generator is shown in *figure D.6.* With the system it is possible to use a single looped conductor for the armature rather than using coils. This however does fix the inductance of the system, unlike coils where the inductance will vary over time. The armature and fixed coil are divided up into many discrete parts. The mesh model takes into account

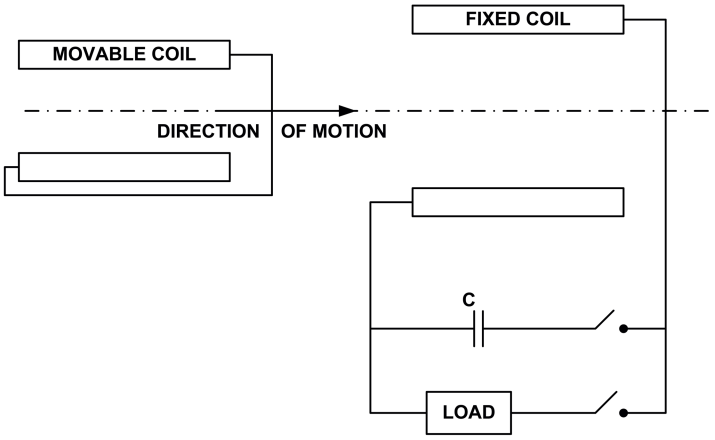


Figure D.6: Generator schematic for a network mesh model [29].

each of these discreet parts and looks at the inductance and resistance of each section. It also looks at how each part interacts with the its neighbouring coils as well as those of the moving armature. The network mesh model used defines three equations which are solved for using the Runge-Kutta method. Reasonably good agreement was reached between the model results and tested device. The physical model parameters are listed below [29].

- Cylindrical tube with an internal diameter of 70 mm
- Fixed coil of 223 μH, 10 $\mu\Omega$ placed over the cylindrical tube
- Copper armature with an external diameter of 69 mm and an internal diameter of 59 mm
- Linear motor used to produce an armature velocity of 25 m/sec

D.5 Summary

The two models presented in this section were developed by Novac and Smith. The simple model was developed to aid in the understanding of FCGs. With this work as well as experiments performed on medium sized generators, the total characteristics of an FCG were quantified and a complete 2D model could be developed. The 2D model breaks the entire generator down into small

components and therefore allows for accurate modelling of a helical FCG. In non-ideal generators there are many losses and these need to be quantified. Results from experimental work in most cases is the only method to determine the effect these losses have on a generator. The next section will provide information on measurement apparatus that are used in FCG experimental work.

Appendix E

The development of models to determine the physical processes during the operation of a flux compression generator accurately, is important. Two such models were presented in the previous section. An ideal model can be developed however correlation with real world generators must be made. This also aids in making the model more accurate as more experiments are performed on different generators. Experimental measurements are required for this and devices used to take measurements in a generator are discussed in this section.

E.1 Measurement devices

In most FCGs the mechanical system relies on detonics; apparatus in this respect will be mentioned. However in the design of a non-explosive system these devices would not be used. There are a couple of devices for measuring the electrical and electromagnetic properties of the generator during its performance; however not all devices will be used on every experiment as those that are used, will often be destroyed.

E.1.1 Magnetic measurement devices

Flux density probes

Magnetic induction probes or B-dot probes are used for the measuring of the flux density in a generator. They are the most common method piece of apparatus used for measuring pulsed magnetic fields [23]. These probes consist

of a simple but accurately calculated number of turns of thin wire. The probe looks at dB/dt which when picked up is placed through an integrator and then into an oscilloscope. Though the simplest to use and having very high bandwidths, there are issues arising in their use. Purely from the nature of the work, very high magnetic fields are produced, which in turn can induce very high emfs in the probes; electrical breakdown and electromagnetic noise are some of the the problems. For very high magnetic field generators there are instances where the electromagnetic field can change the geometry of the probes and even melt the wire the probes are made of because of the high currents induced in them [23].

Faraday rotation diagnostics

The principle of Faraday rotation is that polarised light travelling along a magnetic field will undergo rotation if it is in a suitable medium. The rotation angle is proportional to the line integral of the magnetic field in the medium [30]. The Faraday units consists of a single turn of twisted fibre illuminated by a diode laser. This is sent through to quadrature splitters and a pair of photo diode detectors.

E.1.2 Current measurement devices

Rogowski Coils

A Rogowski coil is an air-cored toroidal coil placed round a conductor. The alternating magnetic field produced by the current induces a voltage on the coil which is proportional to the rate of change of current ($V_{coil} = M di/dt$), where the mutual inductance of the coil is $M = \mu n A$. The Rogowski coil has many advantages for measuring current through a conductor [31]:

- Inherently linear
- Excellent transient response
- Flexible design, ideal for difficult to reach places

- Can be designed to be self integrating
- Frequency independent

Construction It is important to construct the Rogowski coil with uniform windings. If the winding is not uniform the the coil can pick-up stray magnetic fields from adjacent conductors and other magnetic sources. The wire should be wrapped around a non-metallic core and have a return conductor down the centre of the coil so that both the ends of the coil are at the same place.

In the case where the coil is not self integrating additional circuitry is required. An integrator as shown in *figure E.1* should be used. The time constant of the integrator is $\tau = CR_c$. Therefore the output from the circuit is:

$$v_{out} = -\frac{1}{\tau}\int v_{coil}\, dt \tag{E.1.1}$$

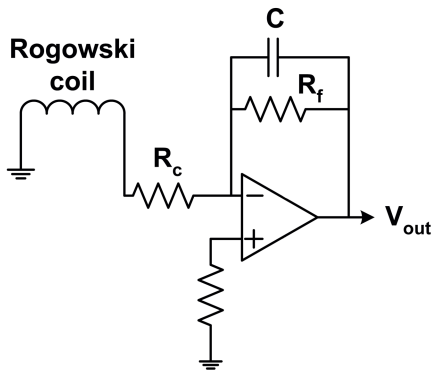


Figure E.1: Rogowski coil and integrating circuitry [31].

E.1.3 Mechanical measurement devices

Velocity interferometer

This has been used on measurements of the Advanced Liner Technology Experiment (ALT-1) in Russia. The velocity interferometer continuously measures the inner surface velocity of the liner throughout its entire travel range [32].

Fibre optic impact pins

These are placed in the stator block to record the impact of the liner and stator. They provide the time, azimuthal and axial symmetry information. When the fibres are struck by the moving liner there is a shock which induces heating at the end of the conductor and light is emitted down the fibre. Quasi-logarithmic photomultiplier tubes are used to detect this light and the signal is recorded on a digitizer.

E.1.4 Measuring limitations

In a lot of experiments performed there are issues with the measuring apparatus. Their lifespan is often limited by the explosives used during flux compression or due to heating produced by the the high dB/dt field.

E.2 Summary

The measurement system used in MCGs must be sufficiently robust to collect all data until the device is physically destroyed. Basic devices are generally acceptable to collect the data and also keep the costs down as the measurement devices are usually rendered useless after a single experiment. The magnetic field and liner velocity can in most cases be easily measured and this provides the researcher with useful data for model development and understanding. The use of measurement apparatus helps to develop an understanding of the real world losses experienced in an FCG. These losses will be discussed in the next section.

Appendix F

The measurement devices mentioned in the previous section aid the researcher in accurately determining the actual performance of a generator. This also aids in producing information regarding the losses experienced in a generator. Models based on ideal systems will provide some solution but the inclusion of some of the losses experienced in a generator is important for an accurate evaluation of a generators performance. Knowing the losses can be useful in selecting the most important loss components for model analysis and ignoring the rest. This appendix will highlight most of the important loss mechanisms that occur and will also provide some methods to reduce some of losses.

F.1 Losses

The losses that occur in MCGs can be placed in one of four categories, these can be defined as:

- Magnetic
- Thermal
- Electric
- Mechanical

In a lot of cases there is overlapping of the different losses as one may affect another and the object in any design is to try and reduce all possible losses or reduce the more serious ones for the overall improvement of the generator.

F.2 Magnetic losses

F.2.1 Flux diffusion

The loss of magnetic flux into a conducting wall is seen as one of the most limiting factors for the performance of a flux compression generator [33]. A high value of conductivity, the characteristic of a near perfect conductor produces a system performance close to that of a lossless circuit model. What has been noted in all the work performed with either copper or aluminium is that the difference in performance between the different conductors is only a few percent. In all generators there is a certain amount of flux leakage. This occurs as flux penetrates into the conductor as it is trying to compress the flux. The factors affecting the rate at which the flux leaks through the conductor are:

- The finite resistivity ρ
- The velocity v of the moving conductor

These values set the minimum velocity required to produce a certain field. The process of flux diffusion into thick walled conductors is non-linear [33]. Due to the thick walls the current density distribution is non-uniform, which makes the heating non-uniform and therefore the change of conductivity non-uniform.

The penetration of the flux into a conductor is defined by the skin layer of the conductor, this defined by:

$$\delta = \sqrt{\frac{2}{\omega\mu\sigma}} \tag{F.2.1}$$

where:

- ω is the frequency of the pulsed field
- μ is the magnetic permeability of the conductor
- σ is the conductivity of the conductor

The skin time is defined by:

$$\tau_S = \frac{1}{2}\pi\mu\sigma\delta^2 \tag{F.2.2}$$

which is the time required for the magnetic field to penetrate into the conductor the depth of the skin layer.

F.2.2 Magnetic forces

As the flux is compressed there is an increase in the field strength. This therefore requires that the initial velocity is sufficient to overcome the increasing magnetic force due to the stronger field. It is also a requirement that the time of the compression is short so that the magnetic forces will not affect the conductor surface and therefore cause distortion of the conductor.

F.2.3 Flux pockets

This process occurs when a conducting wall is met by another conducting wall. Often they are of slightly different radii and as a result not all the flux in the smaller radii has been swept out [33].

F.3 Thermal losses

F.3.1 Eddy current losses - temperature rise

The resistivity will cause currents to flow in the conductor, which gives rise to Joule heating of the conductor. If the field gets too high the Joule heating may exceed the conductors melting point and as a result vaporisation of the conductor may occur [22]. In such a case flux compression will cease. Reported fields of 1400 T (14 MG) should have a temperature rise above $10^{5\circ}$ as calculated by Lewin [22]. Lewin did note however that even at these high temperatures the equation of state, of copper, prevent the evaporation of the conductor because of the high pressures involved. Therefore the temperature rise of the conductor does not set the upper limit of the attainable field. Lewin and Smith [22] derive an equation for the maximum temperature of the conductor during flux compression. The heating as mentioned above is related to the distribution

of the current density through the conductor. The temperature is recorded in Kelvin and the equation is defined as:

$$T \sim 1400\, H_f^2 \tag{F.3.1}$$

where H_f has units of MG.

F.4 Electrical losses

F.4.1 High electric fields - electrical breakdown/arcing

If a conductor moves through a magnetic field an electric field is generated at the surface of the conductor. This is defined by:

$$\mathbf{E} = -\mathbf{v} \times \mathbf{B} \tag{F.4.1}$$

If the front of the conductor and the magnetic field are parallel then the magnitude of the electric field is the result of the normal of the velocity of the conductor and the field. However in most cases inside MVGs the liner and current carrying coils are usually at some angle to each other and therefore the electric field strength is defined by:

$$\mathbf{E} = \frac{v\mathbf{B}}{sin\,\alpha} \tag{F.4.2}$$

Electrical breakdown therefore occurs just before liner and conductor make contact and the angle between them is very small. This results in losses of the trapped flux and as a result a loss in total compressible flux in the generator.

F.5 Mechnical losses

F.5.1 Mechanical defects

Imperfections from the construction of a generator can cause a dramatic reduction of performance [7]. The finish of the liner is in most cases unimportant and the liner properties such as roundness and uniformity in thickness is far more critical.

F.5.2 Turn skipping or π-clocking

This occurs usually when the liner is slightly off axis or there is non-uniform expansion. As the liner expands the liner will skip a turn or half turn. This can be avoided with maintaining the construction within a tolerance defined by[7]:

$$\Delta a = \frac{p}{4} tan\theta \tag{F.5.1}$$

where:

- p is the wire pitch
- θ is the expansion angle of the liner

F.5.3 Liner destruction

Under the pressure of the force exerted on the liner by the explosives and the magnetic forces as the field is compressed the liner can be partially or totally destroyed. If this should happen then the trapped flux up to that point will be lost from the system and the compression of the flux of any nature will cease. It is therefore important not to have the compression volume too large. If this does occur and the elastic limit of the liner material is reached the liner will then fracture.

F.6 Dealing with these problems

In Russia they have adopted a new system by which the liner is composed of tiny copper links joined together. This reduces the effects of eddy currents as well as providing more elasticity without interfering with the conductivity of the liner.

F.6.1 Gas in generator volumes

Filling the compression volume with different gases has a varying effect on the processes during compression. If the compression volume is under vacuum and during the operation of the generator there is the emission of metal vapour, this can bring the gas very quickly to the Paschen minimum for breakdown. This therefore aids in the breakdown of the internal high voltages [34]. Noble gases also pose a problem as they have no electronegative component and as a result any electron released during compression is amplified and results in breakdown. In a lot of cases the use of standard air is adequate for most generators. the use of sulfur hexafluoride (SF_6) is used in cases where electrical breakdown is persisting but the molecular mass of SF_6 can cause the armature to slow down during compression.

F.7 Summary

There are four main categories of losses, magnetic, electrical, thermal and mechanical. There is a close relationship between these losses and often one will affect another. In the reduction of one loss mechanism there may also be a reduction of other losses. It is important to remember that mechanical failure will ultimately result in no output as total loss of flux will occur. Electrical breakdown also has a great effect on the maximum output obtainable from a generator. In the next section a theoretical design of a non-explosive flux compression generator will be discussed.

Appendix G

The losses experienced in a generator can be detrimental to its performance. The major losses were highlighted and some methods for reducing these losses were mentioned in the previous section. A theoretical design of a non-explosive flux compression generator will be presented in this section. Based around many of the techniques and methods described in all the previous sections. The advantages of such a generator will be discussed with particular reference to the losses. The generator would ultimately be designed as a mobile unit intended for experimental work at any location.

G.1 Non-explosive magnetic compression generator

There are many different types of magnetic compression generators, each having its own purpose. However they all require a high energy density device, either in the form of high explosives or from a large capacitor bank. For research in a fixed laboratory with the availability of space and power supply there are no problems for such devices. Besides the design for land mine detection no MCGs are used in outdoor environments other then those detonated in outdoor test facilities. The aim therefore is for the development of a non-explosive MCG which is able to be independent of a lab facility. The output is an electrical impulse from a non-destructive flux compression generator.

The understanding of flux compression and what constitutes flux compression is important in this design, taking the fundamental concept of flux conservation. If the inductance can instantaneously change will the corresponding

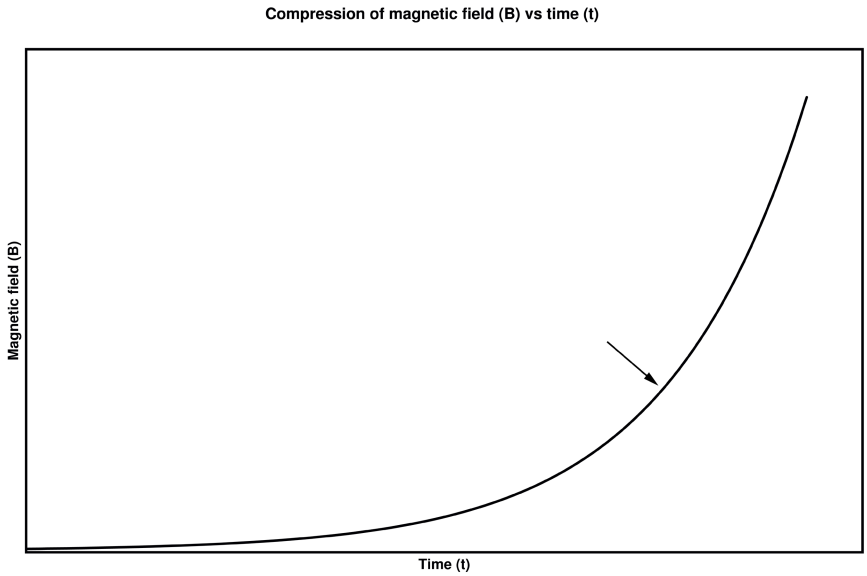


Figure G.1: Graph showing the field strength during flux compression.

current increase? The answer should be yes, as long as there is no electrical breakdown during the process. But does this in fact constitute flux compression. The volume containing the magnetic field has not changed and therefore the answer here should be no.

The volume therefore needs to be changed but to what magnitude? In the case of the generation of high magnetic fields the maximum compression is required for the highest possible field. In the case of producing an electrical impulse the volume does not have to be completely compressed. This is an advantage to the system as this reduces the chance of electrical breakdown as well as clocking of the turns. It requires less initial energy being placed on a liner as the magnetic pressure produced is a lot smaller then those generated in high field generating experiments. The graph in *figure G.1* shows the change in magnetic field during the compression of a volume. The arrow indicates an area providing some compression but limiting the magnetic forces on the material of the generator, therefore requiring less initial force on the liner for flux compression.
There is however still a need for a change in inductance otherwise the output current would be negligible. Therefore a second mechanical or electrical component must be added to the system in order to obtain a change of inductance and therefore a useful impulse output.

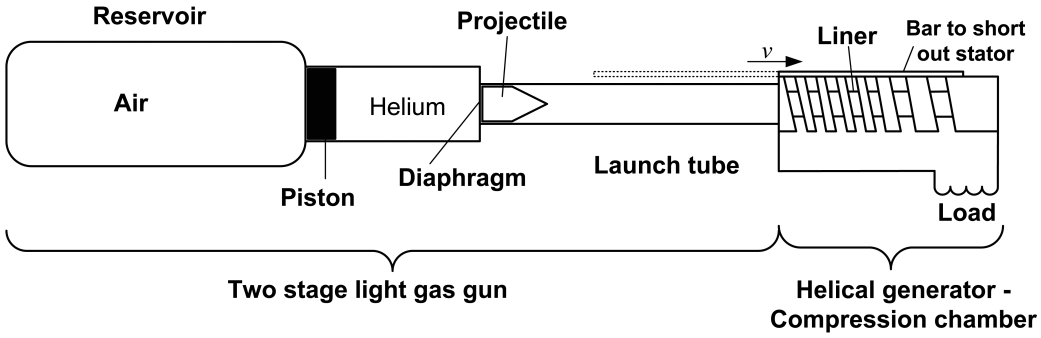


Figure G.2: Schematic of non-explosive flux compression generator design.

G.2 The design

Figure G.2 shows the schematic of the design for a non-explosive flux compressor. The operation is much the same as most flux compressors and is given below:

- Reservoir is filled
- Capacitor bank is charged
- Piston compresses helium
- Capacitor bank discharges into helical coil, setting up primary field
- Projectile is launched at $\pm 2000\, m/s$
- Liner is radially expanded, compressing the volume
- Actuator shorts helical coils, reducing the inductance of the system
- Impulse is delivered to the load

Providing sufficient mechanical energy into the system is one of the biggest issues facing this type of design. However because only partial chamber compression is required, this initial energy value can therefore be lower than in most generators. The energy required for the change of inductance will be provided in the form of a capacitor bank and an electrical actuator to short out the helical coils. Another mechanism is to have a second two stage light-gas gun to launch a second projectile which would short out the coils of the stator section. Each section of the design will be discussed below.

G.2.1 Two stage light gas gun

A two stage light gas gun is the preferred choice for this work. It does not require explosives but can still provide high projectile velocities. Two stage gas guns are generally used for supersonic applications and single stage gas guns are used for subsonic tests. The initial reservoir will be filled with compressed air. The second stage will be filled with helium, which will drive the projectile into the flux compression chamber. Helium is used as it has a higher speed of sound when heated and therefore a higher projectile velocity can be obtained.

G.2.2 Flux compression generator design

The compression chamber will have a copper liner and the stator coil will be a helical coil also made of copper. Copper was selected over aluminium as the difference in their performance is minimal with regard to the compressing of flux. Copper is also a harder metal and therefore less susceptible to fatigue fractures. The field generation and primary current in the stator will be produced by a capacitor bank. The liner will expand to reduce the original volume between the stator and liner by approximately 50 %.

The liner if made with sliding plates rather than a single copper tube will not cause a significant decrease in the projectile's velocity. This would therefore mean there should be quite a uniform liner acceleration towards the stator. The design of such a liner is shown in *figure G.3*. An air gap is shown in the

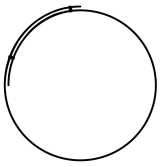


Figure G.3: Diagram of the liner to be used in the generator.

diagram. However for the constructed model the excess material would be in contact over the entire area, therefore aiding in the conductivity of the liner. This design would also allow for multiple uses of such a liner. This is in a similar idea to the chain mail liner mentioned earlier.

The launch tube of the gas gun will be fixed flush with the entrance to the

generator volume. This is to maximise the projectile kinetic energy entering the compression chamber. This will also aid in having a small amount of force from the compression volume still having an effect on the projectile.

The external device to short out the helical coils has an important role in reducing the inductance of the generator but it also has some major problems. The most prominent problem is electrical breakdown between the sliding rod and stator coils. This would have a large effect on the final current that can be produced. The sliding rod therefore needs to close at a very high velocity in order to prevent this. The sliding rod and stator coil will also have a large amount of frictional wear and therefore will need replacing over time.

The external capacitor bank used for the seed field will need power which again in the lab facilities is not a problem. In a remote location a generator and small transformer could be used to charge the capacitors. Though this might be bulky in a redesign it could be reduced for specific applications.

G.3 Design advantages

Flux compression generators are renowned for being small devices for impulse generation. The fact that most generators rely on HE limits the possible areas for detonation. The use of a gas gun therefore allows for the operation of the generator anywhere. The initial size of the gas gun would be large as test facilities are available however in refining the design a small gas gun set-up would be possible, therefore making the unit smaller.

The movement of the liner is limited to half the volume of the compression volume. The fact that the liner and stator do not come into contact removes the chance of turn skipping as well as electrical breakdown between liner and stator. With the sliding liner design this should reduce the chance of liner destruction. Flux pockets will also not happen because there is no contact between a deformed liner and stator.
The field rise will be of a moderate amount which should aid in lowering the temperature rises due to eddy current heating. The magnetic forces on the liner will also be reduced and as a result the required projectile velocity and energy will be less than required in other systems.

G.4 Summary

The design of a non-explosive flux compression generator is possible. One of the most critical elements is the initial kinetic energy of the projectile and this therefore relating to the liner velocity. However with the liner being easily manipulated and a projectile with a velocity greater then 1500 m/s, flux compression should be possible. The need for only a small percentage of the volume to be compressed will also help to minimise the required mechanical energy input. The design also reduces the possibility of turn skipping and electrical breakdown. This would result in a generator for experiments which are repeatable having a consistent performance. With continued redesign the device could be made sufficiently compact to be transportable and usable in any location.

References

[1] A.D. Sakharov. *Collected scientifc works*. Marcel Dekker, Inc. New York, 1982.

[2] T. Erber and H. G. Latal. Flux compression theories. *Report on Progress in Physics*, 33:1069–1127, 1970.

[3] H. Knoepfel. *Pulsed high magnetic fields*. North-Holland publishing Co, Amsterdam, 1970.

[4] H.E. Knoepfel. *Magnetic fields*. John Wiley & Sons, Inc. New York, 2000.

[5] I.R. Lindemuth, C.A. Ekdahl, C.M. Fowler, R.E. Reinovsky, S.M. Younger, V.K. Chernyshev, V.N. Mokhov, and A.I. Pavlovskii. Us/russian collaboration in high-energy-density physics using high explosive pulsed power: Ultrahigh current experiments, ultrahigh magnetic field applications, and progress toward controlled thermonuclear fusion. *IEEE transactions on plasma science*, 25(6):1357–1371, 1997.

[6] T.G. Engel, W.C. Nunnally, and N.B. VanKirk. Design and development of a noval flux compression generator for landmine detection applications. *IEEE transactions on Magnetics*, 35(1):245–249, 1999.

[7] J.C. Dickens A.A. Neuber. Magentic flux compression generators. *Proceedings of the IEEE*, 92(7):1205–1215, 2004.

[8] E. Schamiloglu, R.J. Barker, M. Gundersen, and A.A. Neuber. Modern pulsed power: Charlie martin and beyond. *Proceedings of the IEEE*, 92(7):1014–1019, 2004.

[9] B.E. Kane, A.S. Dzurak, G.R. Facer, R.G. Clark, R.P. Starrett, A. Skougarevsky, and N.E. Lumpkin. Measurement instrumentation for electrical transport experiments in extreme pulsed magnetic fields generated

by flux compression. *Review of scientific instruments*, 68(10):3843–3860, 1997.

[10] T.G. Engel, W.C. Nunnally, and N.B. VanKirk. Compact kinetic-to-electrical energy conversion.

[11] J.P. VanDevender. Prolog to: The special section on pulsed power technology. *Proceedings of the IEEE*, 80(6):931–933, 1992.

[12] M.V. Fazio and H.C. Kirbie. Ultracompact pulsed power. *Proceedings of the IEEE*, 92(7):1197–1204, 2004.

[13] U. E. Israelsson and D. M. Strayer. Flux compression measurements in sintered bulk $ba_2ycu_3o_7$. *IEEE transactions on magnetics*, 27(2):1170–1173, march 1991.

[14] D.C. Giancoli. *Physics for scientists and engineers*, volume second edition. Prentice hall, New Jersey, 1989.

[15] L.W. Matsch and J.D. Morgan. *Electromagnetic and electromechanical machines*. John Wiley & sons, New York, 3rd edition edition, 1987.

[16] M.C. Thompson. Inductance calculation techniques - part ii: Approximations and handbook methods. *Power control and intelligent motion*, December 1999.

[17] G. R. Turner. Inductance calculations for helical magnetocumulative generators. *From NECSA, still to be published*.

[18] B.M. Novac, I.R. Smith, H.R. Stewardson, P. Senior, V.V. Vadher, and M.C. Enache. Design, construction and testing of explosive-driven helical generators. *Journal of physics D: Applied Physics*, 28:807–823, 1995.

[19] R.D. Zucker. *Fundamentals of gas dynamics*. Matrix publishers Inc., 1977.

[20] Con Doolan. A two-stage light gas gun for the study of high speed impact in propellants. Technical report, Weapons systems division Aeronautical and Maritime research laboratory, 2001.

[21] N.K. Bourne. A 50 mm bore gas gun for dynamic loading of materials and structures. *Measurement science and technology*, 14:273–278, 2003.

[22] J.D. Lewin and P.F. Smith. Production of very high magnetic fields by flux compression. *The review of scientific instruments*, 35(5):541–548, May 1964.

[23] L. L. Altgilbers, M.D.J. Brown, I. Grishnaev, B.M. Novac, I.R. Smith, I. Tkach, and Y. Tkach. *Magnetocumulative Generators*. Springer-Verlag New York, 2000.

[24] V. Namias. Induced current effects in faraday's law and introduction to flux compression theories. *American Journal of physics*, 54(1):57–69, January 1986.

[25] D. Kachilla, F. Herlach, and T. Erber. Electromagneticaly driven flux compression. *The review of scientific instruments*, 41(1):1–7, January 1970.

[26] E. Levi, Z. Zabar, and L. Birenbaum. Basic performance of flux-compression/expansion electromechanical converters. *IEEE transactions on plasma scence*, 20(5):554–561, 1992.

[27] B.M. Novac, I.R. Smith, M.C. Enache, and H.R. Stewardson. Simple 2d model for helical flux-compression generators. *Laser and Particle beams*, 15(3):379–395, 1997.

[28] B.M. Novac, I.R. Smith, M.C. Enache, and H.R. Stewardson. 2d modeling of inductively coupled helical flux-compression generators - fluxar systems. *Laser and particle beams*, 15(3):397–412, 1997.

[29] B. Azzerboni, E. Cardelli, and M. Raugi. A network mesh model for flux compression generators analysis. *IEEE transactions on magnetics*, 27(5):3951–3954, 1991.

[30] L.R. Veeser, P.J. Rodriguez, B.R. Marshall, W. Lewis, and O.M. Tatsenko. Optical magnetic field diagnostics for the mc1 flux compression generator experiments. *Digest of technical papers - IEEE international pulsed power conference*, pages 1058–1062, 1995.

[31] D.A. Ward and J.L.T. Exon. Using rogowski coils for transient current measurements. *Engineering science and educational journal*, pages 105 – 113, 1993.

[32] D.A. Clark, B.G. Anderson, G. Rodriguz, J.L. Stokes, and L.J. Tabaka. Liner velocity, current and symetry measurements on the 32 mega-amp flux compression generator experiemnt alt-1. *IEEE international conference on plasma science*, pages 1390–1393, 2001.

[33] R.E. Reinovsky and I.R. Lindemuth. Design considerations for 100 mj class flux compression pulse power systems. *Digest of technical papers - IEEE international pulsed power conference*, pages 329–332, 1993.

[34] A. Neuber, T. Holt, J.C. Dickens, and M. Kristiansen. Thermodynamic state of the magnetic flux compression generator volume. *IEEE transactions on plasma science*, 30(5), 2002.